

A STUDY OF SABOT DECELERATION BEHIND AN AERODYNAMIC  
VEHICLE IN A GAS-FILLED TUBE

by

CARL STEPHEN ENGELBRECHT

A thesis submitted in partial fulfillment  
of the requirements for the degree of

Master of Science in Aeronautics and Astronautics

University of Washington

1986

Approved by



(Chairperson of Supervisory Committee)

Program Authorized

to Offer Degree

Department of Aeronautics and Astronautics

Date

In presenting this thesis in partial fulfillment of the requirements for a Master's degree at the University of Washington, I agree that the Library shall make its copies freely available for inspection. I further agree that extensive copying of this thesis is allowable only for scholarly purposes, consistent with "fair use" as prescribed in the U.S. Copyright Law. Any other reproduction for any purposes or by any means shall not be allowed without my written permission.

Signature \_\_\_\_\_

Date \_\_\_\_\_

University of Washington

Abstract

A STUDY OF SABOT DECELERATION BEHIND AN AERODYNAMIC  
VEHICLE IN A GAS-FILLED TUBE

by Carl Stephen Engelbrecht

Chairperson of the Supervisory Committee:  
Professor Abraham Hertzberg  
Department of Aeronautics and Astronautics

The concept of using a closed tube filled with a heavy gas to separate a vehicle from its sabot is studied theoretically. The accuracy of the theoretical model is verified by experimental tests. Vehicle and sabot enter this "sabot stripper" together and must, to be useful, exit at least 1 meter apart. Acceptable vehicle exit velocities are above 1000 m/s for a launch velocity of 1100 m/s. Argon and carbon dioxide are examined as candidate gases in a system with a 12 ft. long tube, a 72 gm vehicle and a 37 gm sabot.

Argon theoretically yielded a vehicle velocity of 941 m/s at its exit from the sabot stripping tube. At this time, the vehicle was 1.33 meters ahead of the sabot. This distance is traversed by the sabot, which exits the tube at 326 m/s, in 3.6 ms. The inadequate final vehicle velocity is a result of the flow over the vehicle being unstirred due to the sabot shock catching up with and passing the vehicle.

Experimental tests reveal that the theoretical prediction of vehicle behavior is accurate to within 1.5%. This error is defined as the difference between the theoretical and actual exit times divided by the actual exit time. However, because of the simplicity of the model used, the prediction of sabot behavior is 20% in error.

To keep the sabot shock from catching the vehicle, a gas with a lower shock speed is sought. This gas should also have a similar molecular weight to maintain adequate sabot deceleration.  $\text{CO}_2$  is selected, and in it, the flow over the vehicle remains started throughout the entire sabot stripper. The vehicle velocity is consequently determined to remain essentially unchanged. When the vehicle exits the sabot stripper, the separation between vehicle and sabot is 1.5 m, a distance which takes the sabot 6.3 ms to travel. The sabot exit velocity is 160 m/s. These values are well within the range sought, and  $\text{CO}_2$  is thus found to be a usable gas for this application.

In  $\text{CO}_2$ , the error in predicted vehicle velocity is negligible. Also, because the flows in this case are much simpler than in argon, the sabot behavior is predicted much more accurately. In this case, theory agrees to within 5%.

## TABLE OF CONTENTS

	<u>Page</u>
List of Tables.....	iii
List of Figures.....	iv
List of Plates.....	vi
Chapter I. Introduction.....	1
Chapter II. Theory.....	5
Condition 1.....	11
Condition 1K.....	13
Condition 2.....	15
Condition 3.....	17
Condition 4.....	18
Condition 5.....	20
Condition 5A.....	22
Condition 5B.....	23
Condition 5C.....	24
Condition 5D.....	25
Chapter III. Experimental Apparatus.....	27
Chapter IV. Results.....	40
Argon Test.....	43
Carbon Dioxide Test.....	53
Chapter V. Conclusion.....	61
List of References.....	63
Appendix A. Listing of Output from Data Acquisition System for Argon and CO <sub>2</sub> Tests.....	65
Appendix B. Listing of FORTRAN Program SABOT.....	70

LIST OF TABLES

<u>Number</u>	<u>Page</u>
1. Results of Test with a Sabot Alone to Determine a Value for the Friction Force.....	42
A.1. Positions of Pressure Transducers Downstream from the Beginning of the Test Section.....	65

## LIST OF FIGURES

<u>Number</u>		<u>Page</u>
1.	Relative Positions of Sabot, Vehicle and Normal Shock for Condition 1 Analysis.....	11
2.	Relative Positions of Sabot, Vehicle and Normal Shocks for Condition 1K Analysis.....	14
3.	Relative Positions of Sabot, Vehicle and Normal Shock for Condition 2 Analysis.....	15
4.	Relative Positions of Sabot, Vehicle and Normal Shocks for Condition 3 Analysis.....	16
5.	Relative Positions of Sabot, Vehicle and Normal Shocks for Condition 4 Analysis.....	19
6.	X-T Diagram Showing Times for Conditions 5A, 5B, 5C, and 5D when Vehicle is Preceded by a Shock....	20
7.	X-T Diagram Showing Times for Conditions 5C and 5D when no Shock Precedes Vehicle.....	21
8.	Schematic of the Ram Accelerator Facility.....	28
9.	Cutaway View of a Light Fiber Instrumentation Probe.....	32
10.	Schematic of PIN Photodiode Amplifier Circuit.....	34
11.	Cutaway View of Kistler Pressure Transducer Instrumentation Probe.....	36
12.	Ram Accelerator Vehicle Configuration.....	38
13.	Ram Accelerator Sabot Configuration.....	39
14.	Pressure vs. Time Output of the Argon Test from Pressure Transducer #1.....	44
15.	Pressure vs. Time Output of the Argon Test from Pressure Transducer #2.....	44
16.	Pressure vs. Time Output of the Argon Test from Pressure Transducer #3.....	45
17.	Plot of Results of Experimental Argon Test.....	47
18.	Plot of Results of Theoretical Argon Test.....	48

<u>Number</u>		<u>Page</u>
19.	Comparison of Theoretical and Experimental Characteristics of the Vehicle in Argon.....	50
20.	Comparison of Theoretical and Experimental Characteristics of the Sabot in Argon.....	52
21.	Pressure vs. Time Output of the CO <sub>2</sub> Test from Pressure Transducer #1.....	54
22.	Plot of Results of Experimental CO <sub>2</sub> Test.....	55
23.	Plot of Results of Theoretical CO <sub>2</sub> Test.....	57
24.	Comparison of Theoretical and Experimental Characteristics of the Sabot in CO <sub>2</sub> .....	58



LIST OF PLATES

<u>Number</u>		<u>Page</u>
I.	The Ram Accelerator Facility seen from the Final Dump Tank, Showing (Left to Right) the Final Dump Tank, the Test Section with Data Acquisition System, the Two Preliminary Dump Tanks, the Launch Tube, and the Breech.....	29
II.	The Ram Accelerator Test Section Showing Laser-Fiber Optic and Kistler Pressure Transducer Instrumentation Ports.....	29
III.	Spark Photograph of CO <sub>2</sub> Test Vehicle.....	60
IV.	A Clearer Spark Photograph of a Ram Accelerator Vehicle.....	60

## ACKNOWLEDGMENTS

The author wishes to thank his faculty advisor, Professor Abraham Hertzberg, for his invaluable advice and guidance. The indispensable assistance of Professor Adam Bruckner and Dr. David W. Bogdanoff is also greatly appreciated.

The author gives special thanks to his fellow Research Assistants for their help in running the experiments presented herein. They are: Carl Knowlen, Dean Brackett, Ivan Stonich, Keith McFall and Dale Barr. Much gratitude is also due to Gregory Harper, Professor Thomas Mattick and Ken Pritchett for their technical assistance, as well as to Mac Saynor, Dennis Peterson, Bill Lowe and Otto Brask for their assistance in the machine shop.

## CHAPTER I

### INTRODUCTION

As higher velocities are achieved through advancing technology, there is a need to describe the relevant phenomena. The ram accelerator, conceived by A. Hertzberg, A.P. Bruckner and D.W. Bogdanoff (Ref. 1), provides a means of obtaining experimental data to aid in the understanding of some of these phenomena. This concept was designed to investigate the fluid dynamic interactions of an aerodynamic vehicle traveling through a tube filled with gas. To do this, the vehicle is accelerated to approximately 1,000 m/sec using a single-stage helium gun. The principles of light gas guns are well described by Siegel (Ref. 2). Accelerating an aerodynamic vehicle with a helium gun, however, requires a sabot to take full advantage of the expanding gas from the driver.

A sabot (a French word which means literally "boot") is a small cylindrical slug which effectively obturates the launch tube, not allowing any of the drive gas to escape around it. The aerodynamic vehicle is placed in front of the sabot; thus, vehicle and sabot initially travel down the launch tube together. If, however, they were to enter the pressurized test section together, a normal shock would immediately be propagated forward by the sabot over the vehicle, thus unstarting the vehicle. Therefore, the

original purpose of the experiment - to investigate what happens to the supersonic flow over the vehicle alone - would not be attained. For this reason, after the vehicle has been accelerated, the sabot, which is now no longer useful, must somehow be slowed to such an extent that when it does reach the test section, its shock will be too slow, and too far behind the vehicle, to have any chance of catching up with it and affecting the flow around it. This sabot stripping must also take place without appreciably slowing the vehicle.

In many guns which use sabots, sabot stripping presents no real problem, because the separation need not take place until the sabot and projectile have left the barrel of the gun. Often the sabot is made up of two or more pieces which, because of centrifugal or aerodynamic forces, fly apart upon leaving the barrel, slowing significantly, as well as departing from the projectile's flight path. An example of one such sabot is the one used by Bless (Ref. 3). In the ram accelerator, however, the vehicle and sabot do not exit the tube until after their flight through the test section, so these techniques cannot be used.

During the preliminary design phase of the ram accelerator apparatus, it was decided to use fluid mechanical techniques which take advantage of the greater cross-sectional area and smaller mass of the sabot to separate it

from the vehicle. Based on advice given by H. Swift of Physics Applications, Inc., it was decided to use a section of tube filled with a pressurized heavy gas separated from the rest of the tube by thin mylar diaphragms as a sabot stripper. The sabot would be separated by the large drag force caused by the normal shock wave it would propagate forward, while the heavier and streamlined vehicle would continue on, slowed only slightly. Questions were immediately raised, however, as to how large or small the change in the vehicle velocity would be. Even if the flow over the vehicle was initially "started," that is, if the flow over the vehicle was not choked, and was everywhere supersonic, the shock from the sabot could catch and pass the vehicle, resulting in a Kantrowitz unstart\* as the sabot slowed down, significantly increasing the projectile drag. Or, the vehicle might not even Kantrowitz start at all, and thus push a shock of its own forward. Therefore, although it was obvious that the sabot could effectively be slowed using this technique, it was not at all clear that the vehicle's speed would remain in the usable range.

In this thesis, the fluid mechanics in the sabot stripper are investigated both theoretically and experimentally. Exact values of sabot and vehicle

---

\*A Kantrowitz unstart occurs when the flow at a throat created between the vehicle and the tube wall is choked. This results in a constriction of the flow, causing a normal shock wave to be propagated forward.

velocities leaving the sabot stripper are not needed - rather, values that are within a certain desirable range are sought. Therefore, approximations are utilized in the interest of simplicity to result in usable, though not exact, theoretical predictions of the value of sabot and vehicle exit conditions. Experimental tests are run to check the validity of these predictions. This thesis presents a theory which has been verified by experimental results presented here to determine the merits of this type of sabot stripper, and to identify a gas which makes it work well enough to meet the needs of the ram accelerator project.

## CHAPTER II

### THEORY

The basic method of analysis used to create the theoretical model is simple, quasi-steady, one-dimensional, ideal gas dynamics (Ref. 4, Chs. 4 and 5). The actual flows involved are not steady, and computational fluid dynamics techniques applied to this problem would have resulted in a more accurate model. This additional accuracy is, however, not sufficient to warrant the additional complication, so the much simpler quasi-steady technique was selected.

All of the calculations were carried out in the FORTRAN program SABOT presented in Appendix B, using a process of stepping in time. At a given time, conditions were assumed to be steady, and steady one-dimensional calculations were made to determine the instantaneous drag on the sabot and vehicle. These forces were then assumed constant for a given, small period of time to determine new velocities and new positions at the new time. This process was continued until the vehicle and sabot exited the tube.

To determine the new velocities and positions of the sabot and vehicle, the standard equations for constant acceleration were used. These are:

$$x = x_0 + v_0 dt + \frac{1}{2} A dt^2 \quad (1)$$

and

$$V = V_0 + A dt \quad (2)$$

where  $X$  is the distance traveled down the tube,  $X_0$  is the initial distance,  $V$  is the velocity,  $V_0$  is the initial velocity,  $A$  is a constant acceleration, given by force/mass, and  $dt$  is the amount of time the acceleration is applied.

The ram accelerator vehicle has a pointed nose, and its cross-sectional area increases steadily until it reaches a maximum value. At this point, there is a minimum flow area between the vehicle and the tube walls, possibly resulting in a throat. The cross-sectional area then steadily decreases, expanding the flow. The flow is not, however, smoothly expanded to the full tube area. This is because a certain amount of cross-sectional area at the back end of the vehicle is required to survive the large g-forces of launch. Therefore, the back of the vehicle is blunt, resulting in a complicated, and far from isentropic, wake. For simplicity, however, the assumption will be made that, unless there is a shock wave on the vehicle, the flow over it is always considered isentropic, and when there is a shock, the flow is considered to be isentropic everywhere except at the shock. This assumption is not expected to significantly affect the final results, as the cross-sectional area of the tail of the vehicle is relatively



small. The 1-D steady equations for isentropic flow of a perfect gas are:

$$\frac{a_0}{a} = \sqrt{1 + \frac{(\gamma-1)M^2}{2}} \quad (3)$$

$$\frac{P_0}{P} = \left[ 1 + \frac{(\gamma-1)M^2}{2} \right]^{\left(\frac{\gamma}{\gamma-1}\right)} \quad (4)$$

$$\frac{\rho_0}{\rho} = \left[ 1 + \frac{(\gamma-1)M^2}{2} \right]^{\left(\frac{1}{\gamma-1}\right)} \quad (5)$$

$$\frac{A}{A^*} = \frac{1}{M} \left[ \left(\frac{2}{\gamma+1}\right) \left(1 + \frac{\gamma-1}{2} M^2\right) \right]^{\left[\frac{\gamma+1}{2(\gamma-1)}\right]} \quad (6)$$

where  $a$  is the static speed of sound,  $a_0$  is the stagnation speed of sound,  $P$  is the static pressure,  $P_0$  is the stagnation pressure,  $\rho$  is the static density,  $\rho_0$  is the stagnation density,  $M$  is the flow Mach number,  $\gamma$  is the ratio of specific heats,  $A$  is the flow area, and  $A^*$  is the flow area at the throat between the vehicle and the tube. The Mach number is defined as:

$$M = \frac{V}{a} \quad (7)$$

where  $V$  is the flow velocity and  $a$  is the speed of sound in the flow given by:

$$a = \sqrt{\gamma RT} \quad (8)$$

where R is the specific gas constant.

The 1-D steady flow equations for normal shock waves in a perfect gas are:

$$M_Y = \sqrt{\frac{M_X^2 + \frac{2}{\gamma-1}}{\frac{2\gamma}{\gamma-1} M_X^2 - 1}} \quad (9)$$

$$\frac{P_Y}{P_X} = \frac{1 + \gamma M_X^2}{1 + \gamma M_Y^2} \quad (10)$$

$$\frac{a_Y}{a_X} = \frac{P_Y M_Y}{P_X M_X} \quad (11)$$

$$\frac{\rho_Y}{\rho_X} = \frac{P_Y}{P_X} \left( \frac{a_X}{a_Y} \right)^2 \quad (12)$$

where the y subscript refers to variables after the shock, and the x subscript refers to variables before the shock.

To determine the drag on the vehicle, the following is used:

$$D_V = \left\{ [P_f + (\rho_f V_f^2)] - [P_r + (\rho_r V_r^2)] \right\} A_t \quad (13)$$

where  $D_V$  is the drag on the vehicle,  $A_t$  is the cross-

sectional area of the tube, the f subscript refers to conditions in front of the vehicle, and the r subscript refers to conditions at the rear of the vehicle. This equation neglects the frictional drag on the vehicle. Because the ram accelerator vehicle is made to provide clearance between it and the tube wall, and because there is very little surface area contacting the tube, this approximation is probably acceptable for the vehicle. For the sabot, on the other hand, it is not. Because the sabot, made from Lexan, must obturate the tube, the rear of the sabot is hollowed out so that when the drive gas fills the cavity, the walls of the sabot are pressed firmly against the walls of the tube. This forms what is called a Bridgeman seal, common in high pressure applications. Many such applications are discussed in Ref. 5. To approximately account for the relatively large friction force that results, a constant term can be added to the drag force on the sabot. A usable magnitude for this term can be determined experimentally. The drag on the sabot is thus given as:

$$D_{\text{sab}} = P_f A_{\text{sab}} + F_{\text{frict}} \quad (14)$$

where  $D_{\text{sab}}$  is the total drag on the sabot,  $P_f$  is the pressure on the face of the sabot,  $A_{\text{sab}}$  is its frontal area, and  $F_{\text{frict}}$  is the constant friction term.

The modeling and analysis of the conditions inside of the sabot stripper can be divided into several flow conditions. These conditions follow each other in a natural progression, though each may not occur in every specific case studied.

The analysis begins when the vehicle and sabot enter the sabot stripping section, breaking the diaphragm that keeps the pressurized gas in this section. Conditions in this section are assumed constant and known a priori until disturbed. The sound speed is given by Eqn. 8. Sabot and vehicle are assumed to be together, traveling at identical speeds, and the pressure behind the sabot is assumed to be negligible. Also, no gas is allowed to pass through or around the sabot.

When the vehicle and sabot enter the sabot stripper, one of two things may happen. Either the flow over the vehicle will be started, or it will choke at the throat. There appears to be no straightforward way of predicting which will be the case, so one or the other must be chosen arbitrarily, and then compared to experimental results. This analysis, therefore, provides for either case. Flow condition 1 assumes the flow is started, and condition 1K assumes a Kantrowitz unstart. There is no path in the analysis between conditions 1 and 1K.

Condition 1

The relative positions of the sabot, vehicle and normal shock wave in condition 1 are shown in Fig. 1. Because the flow over the vehicle is started, it is assumed to be isentropic, and hence the drag on the vehicle is assumed to be negligible. In addition, though the normal shock generated by the sabot may in fact be on the shoulder of the vehicle, the vehicle's presence is ignored. This is because a quasi-steady solution is sought, and because of the complex relationships between the shock and the area changes introduced by the vehicle, there may be no such solution for this case. The error introduced by this

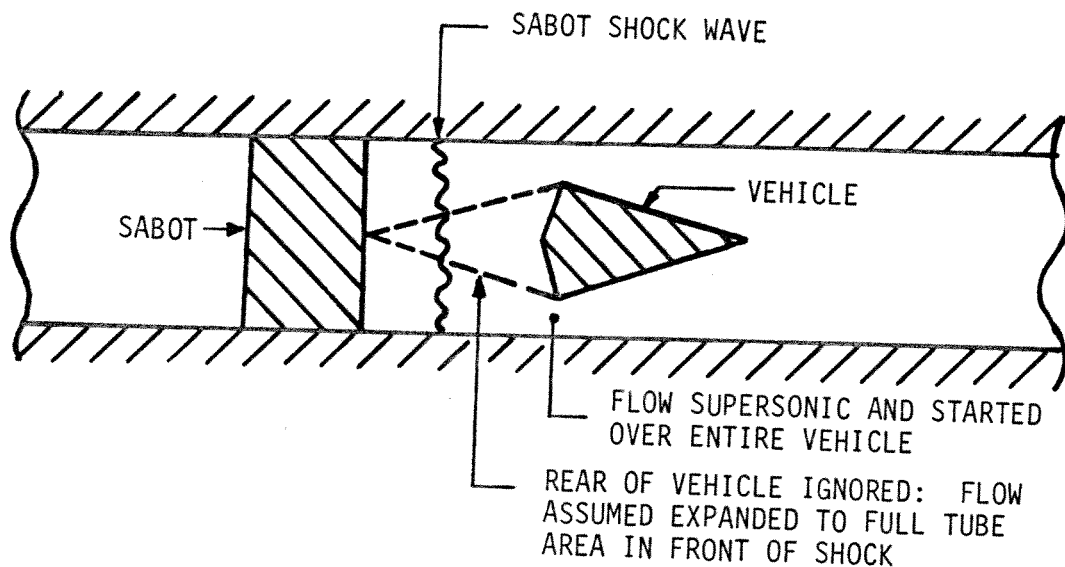


Fig. 1. Relative Positions of Sabot, Vehicle and Normal Shock for Condition 1 Analysis.

assumption is expected to be small because the shock will probably spend only a short amount of time on the vehicle.

The strength of the normal shock is determined by the velocity of the sabot. Because no flow may pass the sabot, the flow in front of the sabot must be moving at the same velocity as the sabot. Therefore, the Mach number of the shock is determined by guessing a value, determining the Mach number behind the shock using Eqn. 9, the sound speed behind the shock using Eqn. 11 and Eqn. 8, and then the speed of the flow using Eqn. 7. This speed is then put into the tube frame of reference and compared with the sabot speed. Iteration continues until they match. The iteration technique chosen is the method of halving. With good initial guesses, this method gives solutions to within 0.1% after usually less than 10 iterations. The pressure ratio across the shock can then be determined, along with the drag on the sabot using Eqns. 10 and 14.

Analysis continues in this phase until the shock catches up with the throat of the vehicle. At this time, the shock is "spit" forward by the vehicle and the system enters condition 2, with the position of the shock coinciding with the nose of the vehicle. If the shock never reaches the throat, the analysis remains in condition 1 until the vehicle leaves the sabot stripper. When this happens, the analysis proceeds to condition 5C, explained below.

Condition 1K

The relative positions of shocks, vehicle and sabot for condition 1K are shown in Fig. 2. Because the vehicle is unstarted, it must, like the sabot, propagate a normal shock wave. The strength of this shock is determined by the subsonic critical Mach number of the vehicle, and therefore by its area ratio.\* A value for the shock Mach number is guessed, yielding through Eqns. 7, 8, 9 and 11 the speed over the nose of the vehicle, and because static values do not change with frame of reference, a flow Mach number using the sound speed behind the shock. This value is compared to the subsonic critical Mach number of the vehicle, and iteration continues until they match.

Because the flow is choked and subsequently becomes supersonic, there must be a second normal shock behind the vehicle and in front of the sabot. Here, as in condition 1, the rear half of the vehicle must be ignored for the sake of maintaining quasi-steady flow, i.e., the flow is assumed to be isentropically expanded to the full tube area immediately behind the throat and in front of the

\*Here, "subsonic critical Mach number" refers to the subsonic Mach number at the vehicle's nose which results in the flow being choked at the throat. It is a function of area ratio, and can be determined by solving Eqn. 6 for  $M$ . This equation has two roots, one subsonic and the other supersonic. The supersonic root is the Mach number that will result at the tail of the vehicle if the flow is choked. This will be referred to as the supersonic critical Mach number.

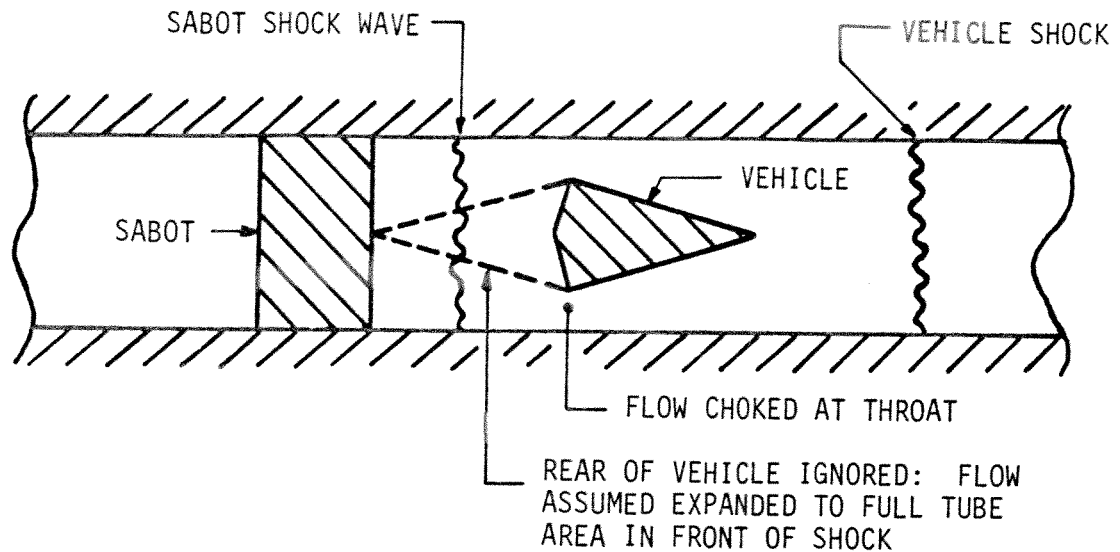


Fig. 2. Relative Positions of Sabot, Vehicle and Normal Shock for Condition 1K Analysis.

second shock to ensure a solution. Because of the large pressure differences between the front and rear of the vehicle, it is extremely unlikely that, after choking, the flow will go subsonic again.

The sound speed in front of the second shock is determined by calculating the sound speed in the stagnation state at the front of the vehicle (Eqn. 3), and using it to calculate the static speed of sound at the vehicle's tail (Eqn. 3). The strength of the second shock can now be determined based on the sabot velocity as was explained above, except in this case the fact that the flow in front of the shock is not at rest must be accounted for. Pressures and densities in front of and behind the vehicle can be found using Eqns. 4, 5, 10, and 12, and the vehicle



drag can be determined using Eqn. 13. The pressure behind the second shock yields the sabot drag (Eqn. 14). These drags are then used to calculate new vehicle and sabot velocities and positions (Eqns. 1 and 2).

When the second shock reaches the throat of the tube, it is "spit" forward and combines with the first shock to form a single shock. At this time, the analysis proceeds to condition 2. If the first shock reaches the end of the sabot stripping tube before this happens, the analysis proceeds instead to condition 5, explained below.

### Condition 2

The relative positions of shocks, vehicle and sabot for condition 2 are shown in Fig. 3. In this case, the propagation velocity of the shock is again determined by the sabot. The flow is therefore subsonic, and hence

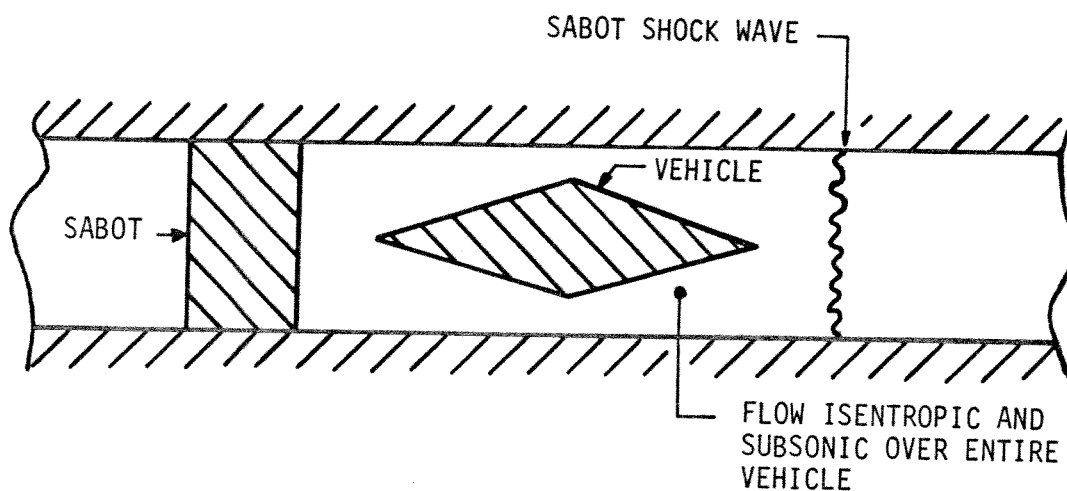


Fig. 3. Relative Positions of Sabot, Vehicle and Normal Shock for Condition 2 Analysis.

isentropic everywhere over the vehicle. The shock velocity is determined, as in condition 1, by iterating until the flow speed relative to the sabot is zero. The speed of the flow at the nose of the vehicle in its frame of reference is the difference between the vehicle and the sabot speeds. Using the known sound speed behind the shock, the Mach number at the vehicle's nose can be calculated. When this Mach number reaches the subsonic critical Mach number, the flow over the vehicle will choke, and condition 2 will no longer be valid. At this time, the analysis proceeds to condition 3. If the difference between the vehicle velocity and sabot velocity is such that the Mach number at the nose of the vehicle is already above the subsonic critical Mach number when condition 2 is initiated, the analysis skips this condition and shifts instead to condition 3. If, however, the Mach number at the nose does not reach the subsonic critical Mach number before the shock wave exits the sabot stripping tube, the analysis will shift to condition 5 below.

Because the flow over the vehicle is isentropic, the drag is assumed to be negligible. The drag on the sabot is calculated using Eqns. 10 and 14. The new vehicle and sabot velocities and positions are calculated using Eqns. 1 and 2.

Condition 3

The relative positions of shocks, vehicle and sabot for condition 3 are shown in Fig. 4. Here, as in condition 1K, the vehicle is choked. Therefore the method for determining the strength of the first shock here is exactly the same as in condition 1K. The position of the second shock is determined iteratively by the condition of no flow through the sabot, as before. This time, however, the area variations introduced by the vehicle must be taken into account. To find the position, and hence the strength, of the second shock, its position (i.e., the ratio between flow area and throat area at its position) must be guessed. Stagnation quantities of pressure, density and sound speed must be calculated in the vehicle's frame of reference from which static quantities can be determined just upstream of

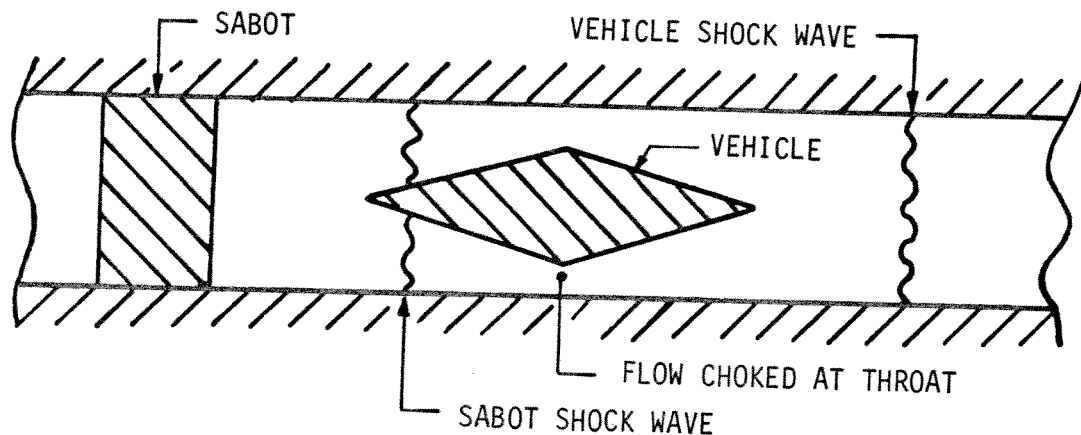


Fig. 4. Relative Positions of Sabot, Vehicle and Normal Shocks for Condition 3 Analysis.

the second shock, using Eqns. 3, 4, and 5. The Mach number of the flow just upstream of the second shock is determined using Eqn. 6. The Mach number behind the shock can then be calculated (Eqn. 9) as well as the new static pressure, density and sound speed, and hence new stagnation quantities (Eqns. 10, 11, 12, 4, 5, and 6). The flow is then further decelerated by expansion, and new flow variables can be calculated at the tail of the vehicle using Eqns. 3, 4, 5, 6, and 7. This flow velocity, after being put into the tube frame of reference, is compared to the sabot velocity, and iteration of shock position continues until they match. After the shock strengths are determined to be correct, the vehicle and sabot drags are calculated using Eqns. 13 and 14, and their new velocities and positions are determined using Eqns. 1 and 2.

If the speed of the sabot is so low relative to the vehicle that no solution for this condition exists, the analysis moves to condition 4; however, if the first shock reaches the end of the sabot stripping tube while condition 3 is still valid, the analysis moves to condition 5.

#### Condition 4

The relative positions of shocks, vehicle and sabot for condition 4 are shown in Fig. 5. As in condition 1K, the flow behind the vehicle is fully expanded before the second shock, but in this case, the second shock's velocity is less than that of the vehicle. Therefore, in this case,

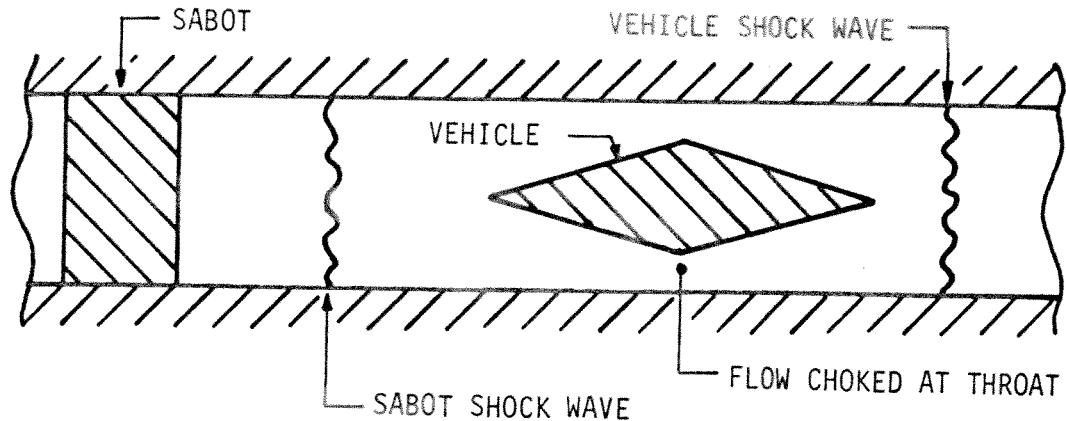


Fig. 5. Relative Positions of Sabot, Vehicle and Normal Shocks for Condition 4 Analysis.

unlike in condition 1K, for relative velocities between the vehicle and sabot larger than in condition 3, there will be a quasi-steady solution. However, because the rear of the vehicle was ignored in condition 1K, the analysis here is exactly the same as it was there. Thus, the shock velocities, sabot and vehicle drags, new velocities and positions can all be determined as in condition 1K.

The analysis has only one path out of condition 4. When the first shock leaves the sabot stripping tube, the analysis moves to condition 5.

Condition 5

Condition 5 is always initiated when the diaphragm at the end of the sabot stripping tube is broken, either by the vehicle itself, if it is started, or by the leading shock. This diaphragm separates the pressurized gas of the sabot stripper from a section of evacuated tube. Thus, when it is broken, the sabot stripping gas will rush out of the tube, and a centered rarefaction fan will propagate upstream at the speed of sound. This further complicates the analysis, prompting the use of additional simplifying approximations. An x-t diagram of what happens to the head of the rarefaction wave, the vehicle, the two shock waves and the sabot is shown in Fig. 6. Further analysis is to

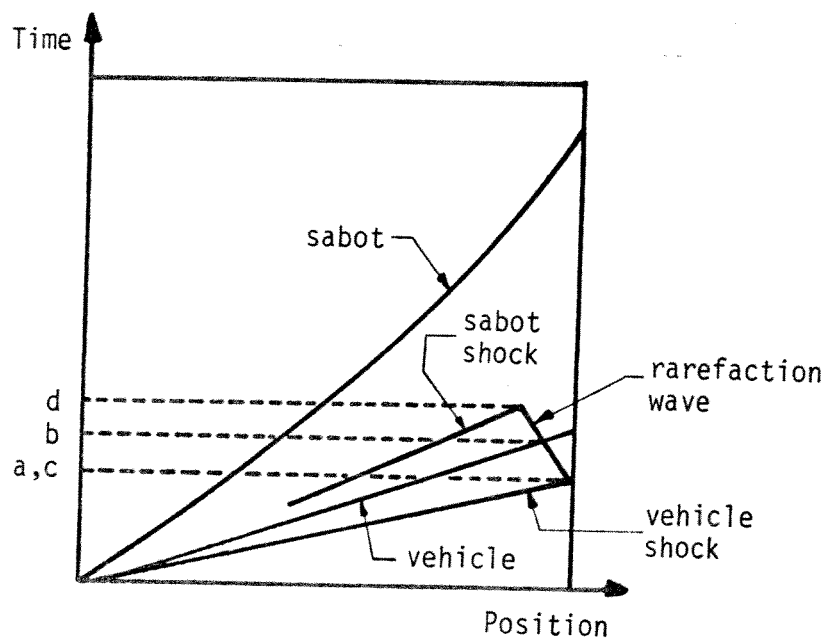


Fig. 6. X-T Diagram Showing Times for Conditions 5A, 5B, 5C, and 5D when the Vehicle is Preceded by a Shock.

be broken down into four additional conditions- two for the vehicle alone and two for the sabot - whose starting points are represented by the letters a, b, c, and d on the time axis of Fig. 6. These letters stand for conditions 5A, 5B, 5C, and 5D.

If the vehicle remains started throughout the tube, the analysis skips conditions 5A and 5B. An x-t diagram showing this condition is shown in Fig. 7.

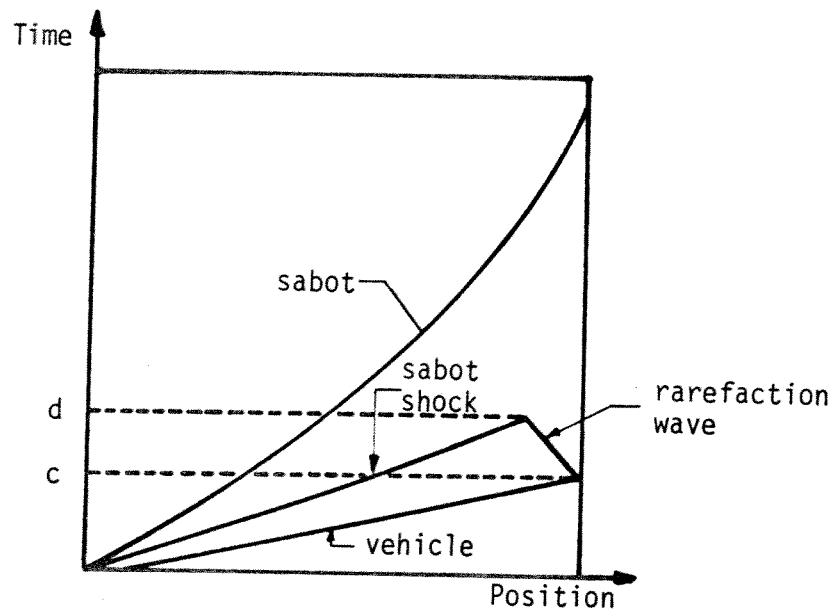


Fig. 7. X-T Diagram Showing Times for Conditions 5C and 5D when no Shock Precedes Vehicle.

Condition 5A

After the shock has exited the sabot stripper, all of the flow in front of the vehicle is subsonic. Thus, for the short amount of time before the rarefaction wave hits the vehicle, the conditions upstream of the vehicle remain constant. The drag does not, however, because it is roughly proportional to the square of the velocity of the vehicle. Thus, in this section no pressures, densities or flow velocities are calculated; rather, the vehicle drag is approximated by:

$$D_v = \frac{F_t (V_t^2)}{(V_{t-dt}^2)} \quad (15)$$

where  $F_t$  and  $V_t$  are the drag on the vehicle and vehicle velocity at time  $t$  respectively, and  $V_{t-dt}$  is the vehicle velocity at time  $t-dt$ . This value can then be used to find the vehicle position and velocity at time  $t+dt$  using Eqns. 1 and 2.

The rarefaction wave is assumed to have a constant speed given by:

$$U_{rar} = a - U_{rel} \quad (16)$$

where  $U_{rar}$  is the velocity of the rarefaction wave,  $a$  is the sound speed behind the shock as it exits the sabot



stripper, and  $U_{rel}$  is the speed of the flow relative to the tube. The rarefaction wave's position is given by:

$$X_{rar} = L_t - (U_{rar} dt) \quad (17)$$

where  $X_{rar}$  is the position of the rarefaction wave,  $L_t$  is the sabot stripper tube length, and  $U_{rar}$  is the rarefaction wave velocity. When the rarefaction wave encounters the vehicle, the analysis switches to condition 5B. The approximations made here are not expected to contribute much to the overall error because the projectile will probably not spend much time in this phase compared to its total flight time.

#### Condition 5B

After the rarefaction wave passes over the vehicle, the flow becomes relatively complicated. An in-depth study of this flow would require analysis beyond the scope of this paper, and would yield results of a much higher accuracy than is needed. Instead, a rather crude, though probably not too inaccurate, assumption that the drag linearly decreases with time to zero at the tube exit is implemented. This assumption will also hopefully have very little effect on the analysis because, once again, of the short amount of time the vehicle spends in this condition relative to the entire time it is in the sabot stripper.

Vehicle position and velocity are calculated as above for each time step.

When the vehicle exits the sabot stripping tube, the analysis moves to condition 5C.

#### Condition 5C

Conditions 5C and 5D are concerned exclusively with the sabot. The analysis in condition 5C depends on which condition the analysis is in when the vehicle exits the sabot stripper. If the analysis proceeded to condition 5 from condition 1, conditions are assumed constant in front of the shock and analysis continues as in condition 1 until the rarefaction wave hits the shock, weakening it. At this time, the analysis moves to condition 5D. This may again seem to be a somewhat extreme approximation but, as in conditions 5A and 5B, the relative time the sabot spends in this condition is small enough to justify it.

If the vehicle left the tube while the analysis was in conditions 1K or 4, the situation is similar. The conditions in front of the second shock are considered to remain constant, and the shock strength is determined iteratively. The vehicle and the first shock are neglected. Once the shock strength is known, the drag, new position, and velocity of the sabot can be determined as before. When the rarefaction wave hits the shock, the analysis moves to condition 5D.

Moving from conditions 2 and 3 presents different problems. If the analysis was in condition 2 when the vehicle left the sabot stripper, it immediately moves to condition 5C. This is because the vehicle's presence is not felt, so this condition is just like a sabot and its shock alone, and the shock has already passed the rarefaction wave.

In condition 3, the second shock is on the shoulder of the vehicle, and the flow in front of it is not fully expanded. If the analysis proceeds to condition 5 from here, the conditions in front of the shock are assumed to be the same as they were in condition 3, except that the flow is assumed fully expanded. Iteration then proceeds as above to determine shock strength and then sabot drag, position and velocity.

#### Condition 5D

As the vehicle does in condition 5B, the sabot enters a very complex flow regime when it becomes involved with the rarefaction waves. Therefore, as in condition 5B, the analysis here simulates the complex interactions between the sabot and its surroundings with a linearly decreasing drag with time. This is the least accurate assumption made in the analysis described here. Its only justification lies in the fact that, if the sabot stripper is working correctly, the sabot speed, when it enters this flow regime, is slow. Therefore, the shock it is propagating

will be weak, and the pressure forces on it will be comparable to or less than the friction forces. Therefore, even as drastic an assumption as the one made here will not nullify the validity of the final result. However, because the sabot is moving slowly in this section, and therefore will spend a relatively large amount of time here, the errors introduced are expected to influence the final result, though hopefully not excessively.

### CHAPTER III

#### EXPERIMENTAL APPARATUS

The apparatus used for this experiment is the ram accelerator facility, shown schematically in Fig. 8. Photographs of the accelerator are shown in Plates I and II. The vehicle is accelerated using a double-diaphragm, single-stage helium gun. These diaphragms are made of 1100-0 aluminum, and scored in a cross pattern. The space between the diaphragms is pressurized to  $2/3$  of breaking pressure, and the breech is filled to  $4/3$  of breaking pressure. Thus, when the gas in the inter-diaphragm space is suddenly released, both diaphragms will burst, applying the breech pressure to the base of the sabot. The 24 ft. long launch tube that the vehicle and sabot travel through initially is evacuated to maximize the vehicle velocity. The launch tube has two pairs of instrumentation ports spaced 1 ft. apart near its end which are used to determine the vehicle velocity after acceleration.

The end of the launch tube is connected to a 5 ft. long perforated tube inside a large evacuated tank which serves as a dump for the drive gas, effectively terminating its influence on the vehicle and sabot. After the helium dump tank, the vehicle and sabot pass through a thin mylar diaphragm into the 8 ft. long sabot stripping section, which, as explained earlier, contains a heavy gas.

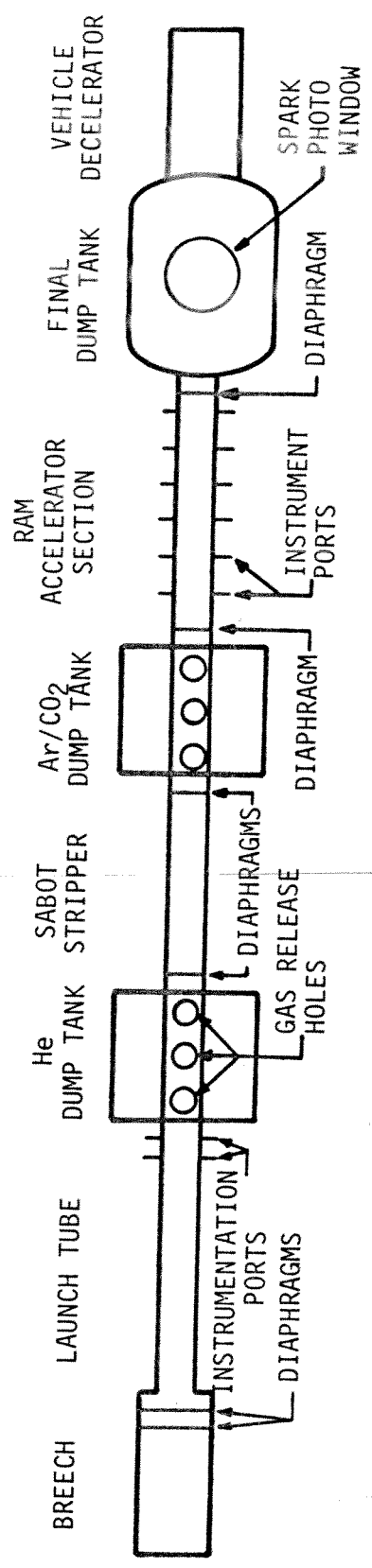


Fig. 8. Schematic of the Ram Accelerator Facility.

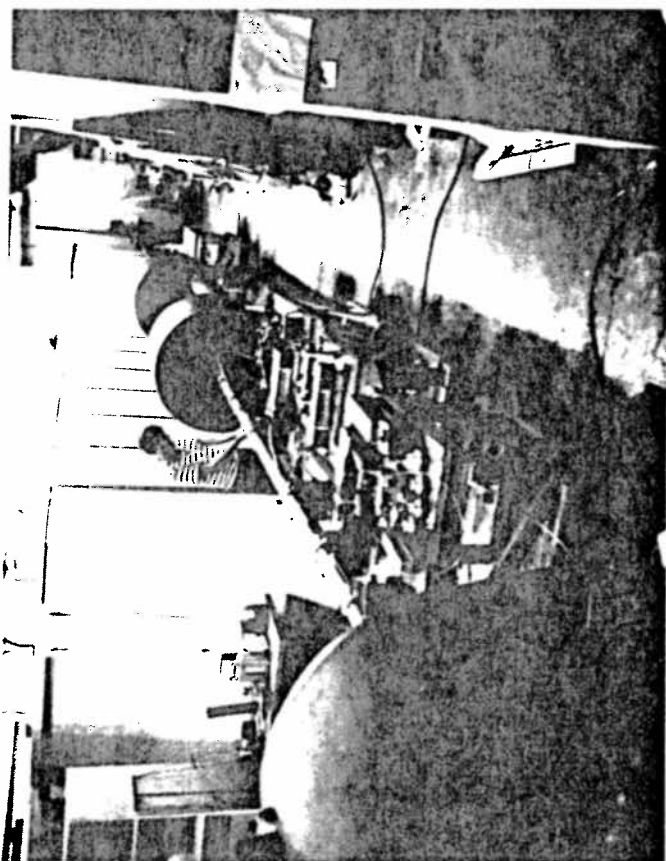


Plate I. The Ram Accelerator Facility seen from the Final Dump Tank, Showing (Left to Right) the Final Dump Tank, the Test Section, with Data Acquisition System, the Two Preliminary Dump Tanks, the Launch Tube and the Breech.

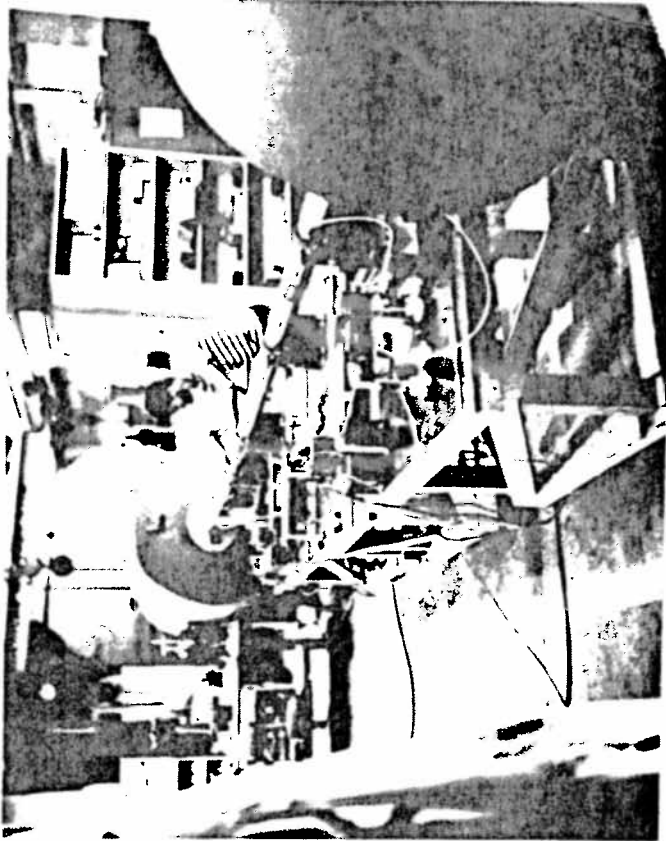


Plate II. The Ram Accelerator Test Section Showing Laser-Fiber Optic and Kistler Pressure Transducer Instrumentation Ports.

After the sabot is stripped, the vehicle (or its shock) breaks a second mylar diaphragm and passes into another 5 ft. long perforated section of tube inside an evacuated tank. The second tank serves as a dump for the sabot stripping gas as well as the drive gas. (The two tanks are connected together by a 10" diameter tube.)

Following the sabot stripper dump tank, the vehicle passes through another mylar diaphragm into the 12 ft. long test section of the tube. This section contains gases whose interactions with the vehicle are to be studied, and therefore, it is equipped with instrumentation ports at several locations along its length. After the test section, the vehicle passes through a third evacuated dump tank, and is brought to an abrupt stop in the vehicle decelerator, which is a large tube filled with lathe turnings.

Because the vehicle is destroyed by its collision with the lathe turnings, no meaningful post-shot examination can be made. For this reason, a spark photography system was installed to take a photograph of the vehicle as it passes through the final dump tank. There is a pair of diametrically opposed 10" dia. Plexiglas windows in the final dump tank to allow the photographs to be taken. The primary reason for this photograph is to determine whether or not the vehicle survives the high stresses involved in



the launch process. Obviously, if the vehicle is destroyed on launch, the data from the shot are meaningless.

Because the primary concern of this thesis is the sabot stripping, and because there is no instrumentation in that section of the apparatus, the tests conducted for this paper were all run with the entire apparatus, except the test section, evacuated. Thus, the test section was used as the sabot stripper, and all analyses in this thesis assume a sabot stripper length of 12 ft.

In the test section, there are eight pairs of instrumentation ports. The first four pairs are placed, starting 1.0 ft. down the tube, at intervals of 2.0 ft. Between the fourth and the fifth pair of ports, there is a space of 17.56 in. The last three pairs of ports follow at 1.0 ft. intervals.

Each pair of instrumentation ports consists of two holes, diametrically opposite each other across the tube. These holes are all threaded identically, so that a variety of data acquisition instruments, when inserted into appropriate plugs, can be fitted interchangeably. These plugs must have a pressure seal which will hold to pressures up to 9,000 psi.

To date, the only types of instrumentation used have been laser-fiber optic velocity probes, and Kistler pressure transducers. The light fiber probes are shown in a cut-away view in Fig. 9. The outside plug is the one

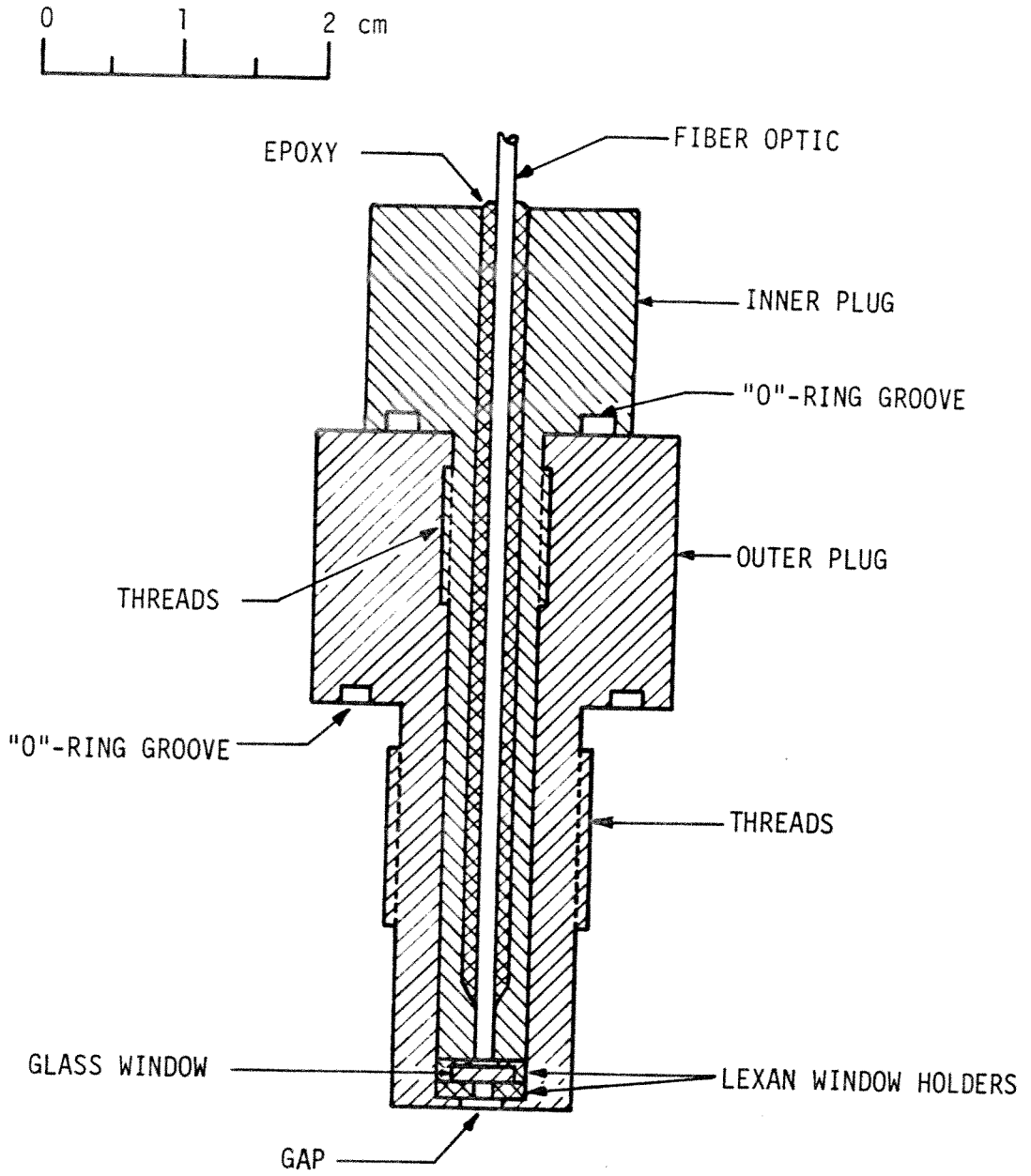


Fig. 9. Cutaway View of a Light Fiber Instrumentation Probe.

which fits into the instrumentation holes in the test section wall. The pressure seal is at the "O"-ring. High tensile strength steel (type 4150) was used to ensure no failure at the threads. The small glass window is used to protect the end of the fiber from any damage, and it in turn is cushioned from shock by the Lexan surrounding it. The seal on the inner plug is provided by its "O"-ring on the outside, and by the epoxy on the inside.

A 2.5 milliwatt laser is used to send light through a 0.059 in. dia. plastic light fiber and across the tube, where it is received by the second fiber optic. This collected light is then transmitted to a PIN photodiode. When the vehicle or sabot pass between the fiber optic ports, the light is obscured, and a change in voltage across the photodiode results. Because the amount of light received by the photodiode is so small, the voltage produced must be amplified considerably to permit reliable data recording. A two-stage amplifier was chosen to keep the frequency response of the photodiode above 1 MHz, the speed deemed necessary to reliably record the passage of the vehicle or sabot. Also, because a positive, high current pulse of about 5 volts is required to consistently trigger the data storage system, the signal must be inverted, and its current amplified. The circuit used to produce a usable signal from the photodiode is shown schematically in Fig. 10.

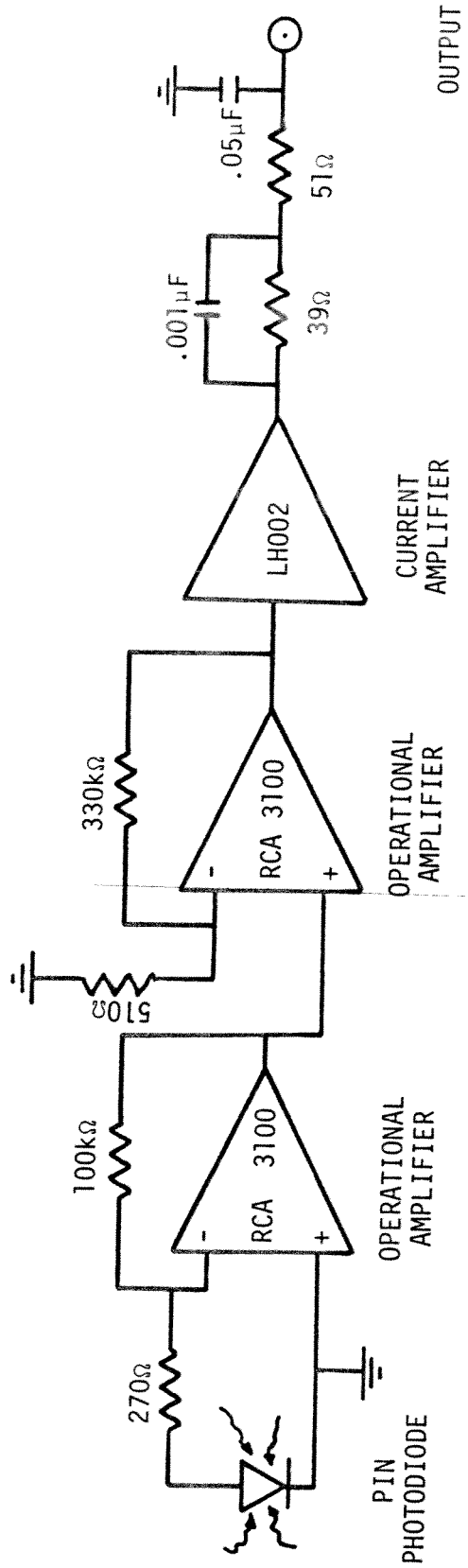


Fig. 10. Schematic of PIN Photodiode Amplifier Circuit.

Pressure measurements were made using Kistler low impedance Type 211B Piezotron pressure transducers, rated at 10,000 psi, mounted in plugs as shown in Fig. 11. A comparison of this figure with Fig. 9 reveals that the external plug has the same geometry as the light fiber plug. The internal pressure seal is provided by the small sleeve at the bottom of the transducer. In order for this to work, the transducer must be pushed downward with a higher force than the one resulting from the maximum pressure on its face. This force is exerted by the two sleeves which surround the transducer. The Microdot connector on the top of the transducer allows it to be connected to a Kistler bias supply and signal conditioner.

All of the information from the light fibers and the pressure transducers is digitized by LeCroy Model 8210 Quad 10-Bit Transient Digitizers, and stored on LeCroy Model 8800 A Memory Modules. These units are mounted on a LeCroy Model 1434 High Powered CAMAC Crate, which is connected to an IBM PC-XT microcomputer, programmed to manipulate and display the data.

Because the PIN photo-diodes are sensitive to infrared radiation, as well as visible light, their signals become difficult to interpret when shock waves and their associated high temperatures are in the vicinity of the vehicle. Therefore, the light detectors were used in the

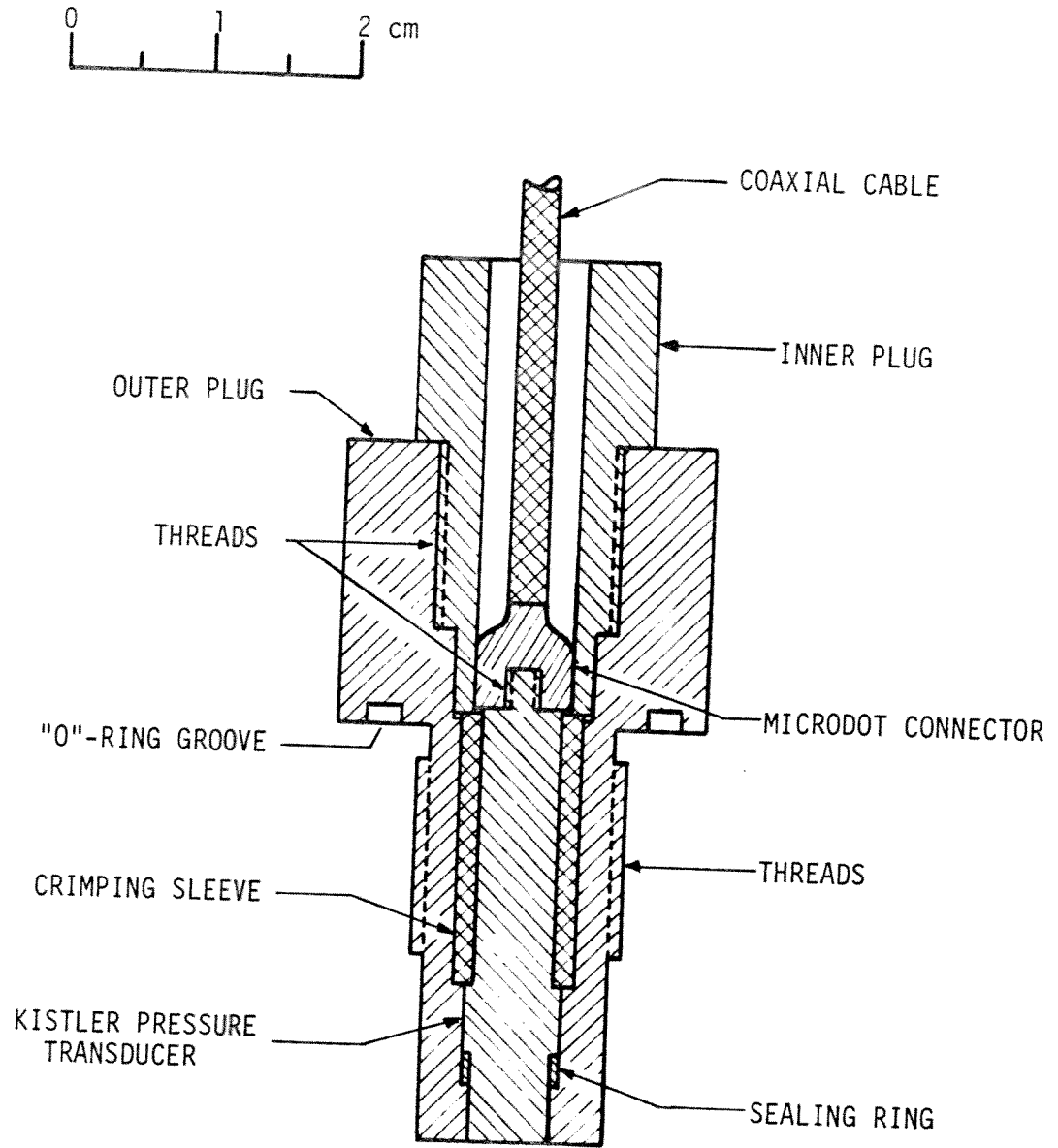


Fig. 11. Cutaway View of Kistler Pressure Transducer Instrumentation Probe.

evacuated launch tube, and the test section was instrumented solely with pressure transducers.

The ram accelerator vehicle is designed to act as a converging-diverging nozzle. It rides in the tube on fins, and is made of magnesium to keep its mass low, about 72g. The nose of the vehicle is a cone having a  $12.5^\circ$  half angle, while the rear is octagonally shaped. The overall length of the vehicle is 13.7 cm. A drawing of the ram accelerator vehicle is shown in Fig. 12.

The sabot is made of Lexan, with a magnesium face plate to protect it from the rear of the vehicle in the high-g field of launch. The rear of the sabot is hollowed out to reduce mass and to allow the drive gas to fill it, expanding the walls to form a Bridgeman seal with the tube walls. Sabots of this type are common. Two similar sabot designs are implemented by Kimura, et al. (Ref. 6) and Ahrens (Ref. 7). A drawing of the ram accelerator sabot is shown in Fig. 13. It is 3.68 cm long, and its mass is 37g.

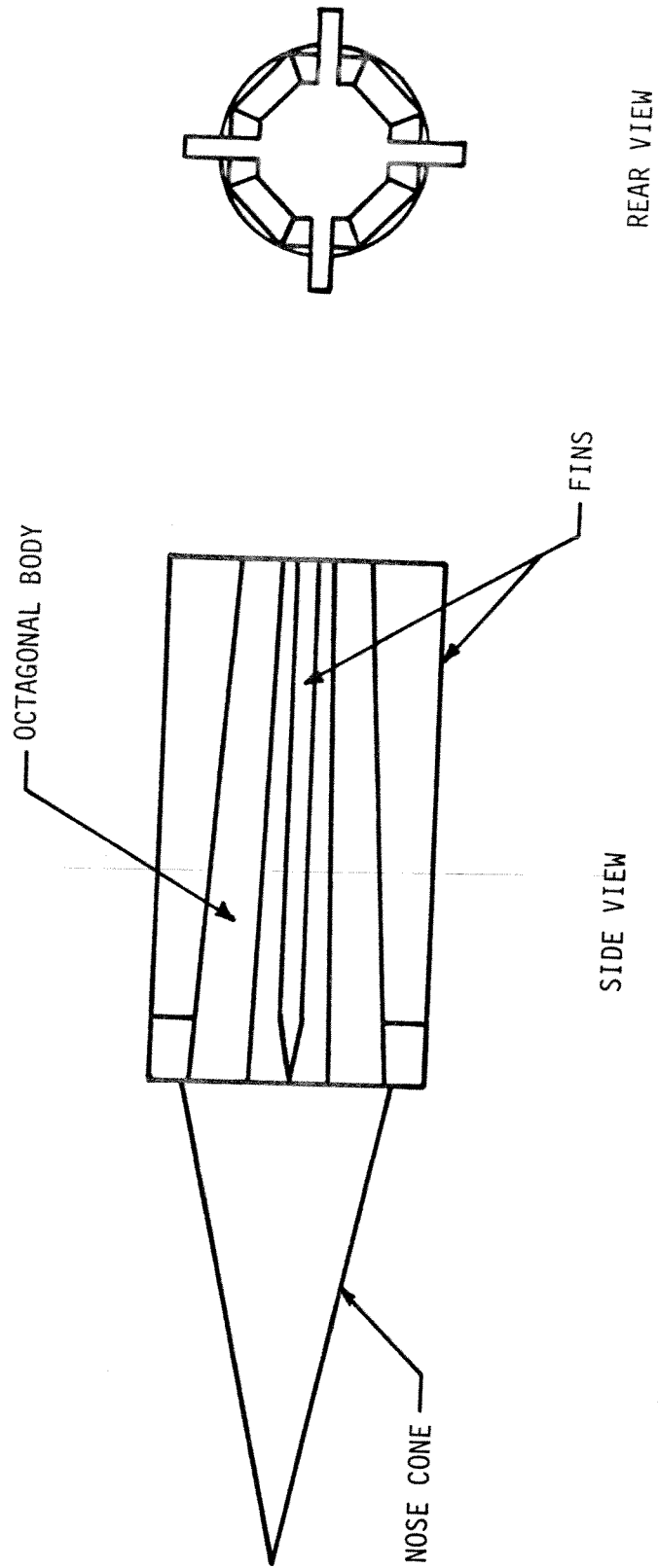
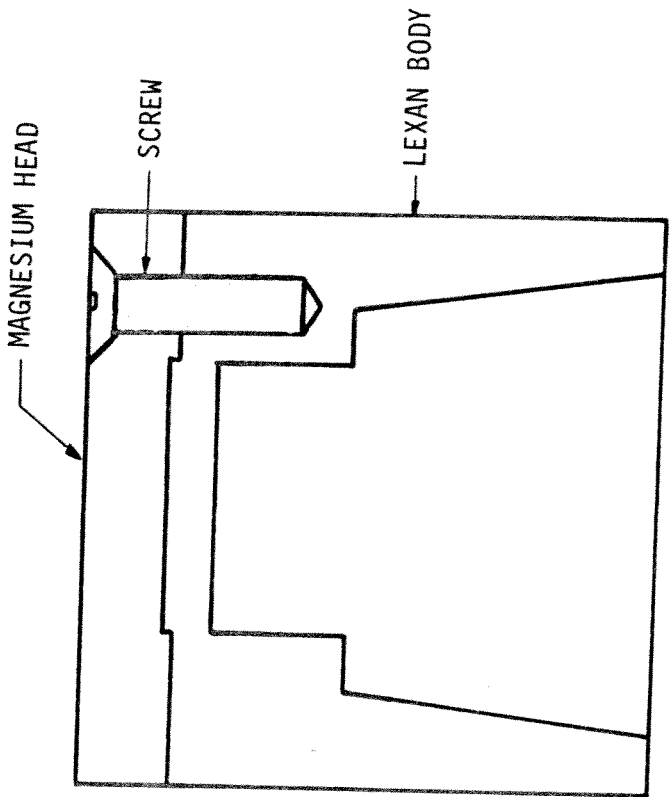
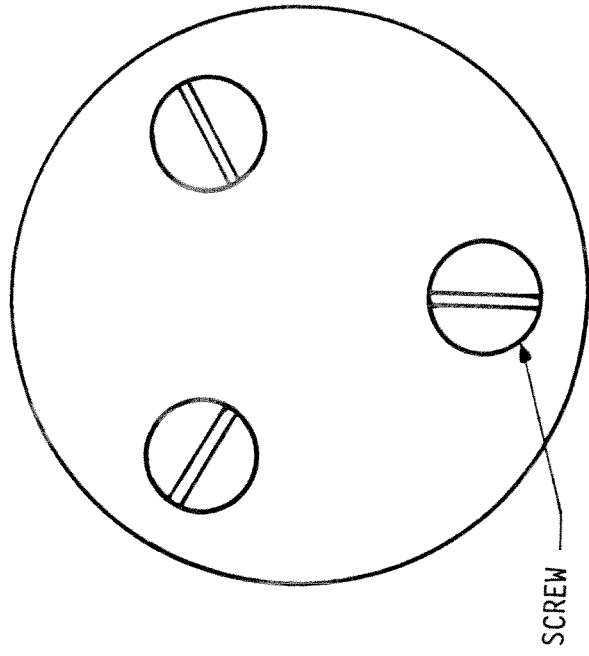


Fig. 12. Ram Accelerator Vehicle Configuration.





CUTAWAY SIDE VIEW



TOP VIEW

Fig. 13. Ram Accelerator Sabot Configuration.

## CHAPTER IV

### RESULTS

To lend merit to any results, a decision must be made regarding the requirements on the sabot stripper. Questions like: "What is an acceptable vehicle exit velocity?" and "What are acceptable sabot exit conditions?" must be answered. A vehicle velocity of 1000 m/s is desired in the test section. Because typical launch speeds are on the order of 1100 m/s, a loss of 10% of the vehicle speed, at most, is acceptable. The required sabot exit conditions are that the sabot must be at least 1 meter behind the vehicle upon exiting the tube, and its shock must not be fast enough to get within 0.5 meters of the vehicle.

Because the work described in this thesis is in support of another, larger project, a working sabot stripper was of primary importance, as opposed to an optimum condition. For this reason, when a successful sabot stripping gas was discovered, the testing was stopped. This was also because the ram accelerator facility was being used for other tests, and because the vehicles are expensive due to a very labor intensive fabrication procedure.

In order to proceed with the analysis, a value for the friction factor of the gun had to be obtained. According to Seigel (Ref. 2, pg. 78), for guns running at velocities comparable to those of this experiment, a typical value for the additional drag on a projectile due to friction and boundary layer effects is 2% of the peak drive force. If all of this drag is assumed to be due to wall friction, it yields a friction force on the order of 500 N for the  $2.5 \times 10^7$  Pa launch pressure of this experiment. The ram accelerator is, however, not a typical gun. Unlike typical light gas guns, it has two five-foot-long sections of perforated tube which can damage the sabot, increasing its drag. Also, Seigel's value is for a metal projectile, not a Lexan sabot. Hence, an experimental value was sought for the sabot friction.

To obtain this, a sabot alone was shot down the tube into argon at 4 atm. Pressures were obtained from the pressure transducers, and the forces caused by these pressures calculated. Velocities were also obtained from the pressure data, since the time of passage of the sabot shows up as a sharp drop in the pressure traces. The pressure release points were plotted on an x-t diagram, and local velocities were determined by taking local tangents to the curve. Hence, the deceleration of the sabot was obtained, and the required force to effect this

deceleration calculated. The difference between these forces is the friction force.

Because the friction force is very small in proportion to the drag when the sabot is moving at high speed, it was decided to use only the data from the last three transducers in order to get as accurate a value as possible. The results of this test are shown in Table 1.

As can be seen, the value for friction force is significant. Also, it appears to be non-constant. Therefore, because the last value is probably the most accurate, for the reasons stated above, the value for the friction force from this test was 1000 N. This is twice the value obtained using the value from Seigel. Because of the crudeness of the experiment, and because of the large discrepancy between values, it was decided to use a compromise between the value obtained experimentally and the theoretical value. The value of friction used henceforth is 750N.

<u>Pressure Transducer #</u>	<u><math>\Delta V</math> (m/s)</u>	<u>Pressure Force (N)</u>	<u>Required Force (N)</u>	<u>Friction Force (N)</u>
6	79.9 m/s	2008	3650	1642
7	76.9 m/s	1595	2815	1220
8	73.95 m/s	1088	2121	1033

Table 1. Results of Test with a Sabot Alone to Determine a Value for the Friction Force.

Argon Test

A sabot and vehicle were shot into 5 atm of argon. The fiber optic probes, which are very good at determining the velocity of nonmetallic slugs, produced indeterminate data as to the velocity at the end of the launch tube, possibly because of sparks or other infrared or visible light produced by interactions between the vehicle and the tube wall. Analysis of the data from the first two pressure transducers, however, yielded a value of approximately 1100 m/s. Because the vehicle is decelerating at this time, however, this value must be considered approximate. The first pressure transducer, 1.0 ft. into the test section, revealed that the first event was the vehicle. This is shown on the pressure vs. time plot from the pressure transducer at station #1 displayed in Fig. 14. Because the vehicle is not preceded by a shock, it is apparent that the flow over the vehicle is started. The shock is, however, on the shoulder of the vehicle.

Between the first and second instrumentation station, the sabot shock overtakes the vehicle, resulting in what is probably subsonic flow over the entire vehicle at station #2. The pressure vs. time plot here is shown in Fig. 15.

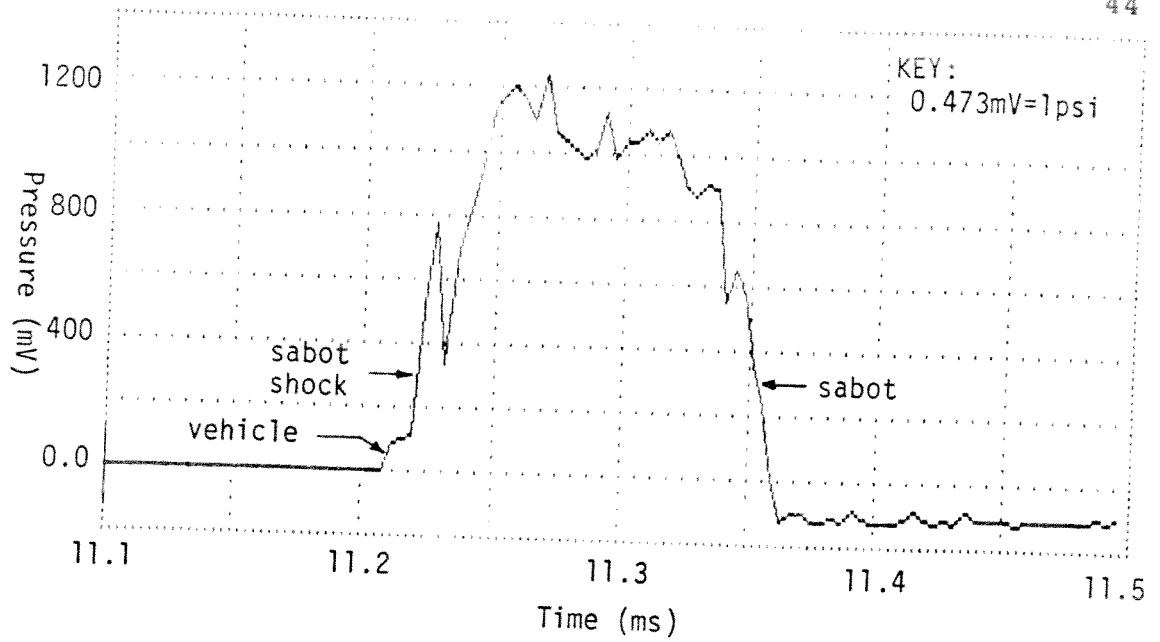


Fig. 14. Pressure vs. Time output of the Argon Test from Pressure Transducer #1.

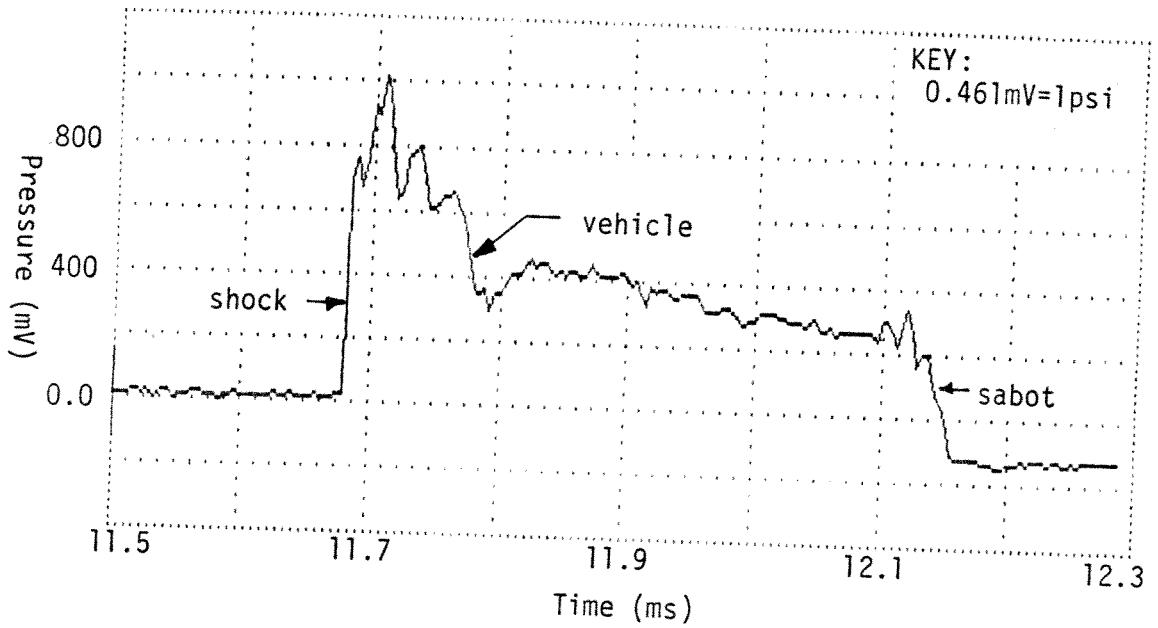


Fig. 15. Pressure vs. Time Output of the Argon Test from Pressure Transducer #2.

At subsequent instrumentation stations, the vehicle becomes quite distinct as a sharply decreasing pressure wave where the flow chokes and accelerates. The positions of the shock and sabot are always obvious. A typical pressure vs. time plot obtained from the data acquisition system for instrumentation ports downstream of station #2 showing shocks, vehicle and sabot is shown in Fig. 16, and the output for the entire test is shown in Appendix A.

It is apparent that the actual flows in the sabot stripper are far from steady. Also, it should be noted that the pressure behind the shocks does not remain constant as assumed. However, the progression of flow states does seem to follow the pattern of the theoretical analysis. At first there is a period of time where vehicle, sabot and shocks are very close together, interacting to such an extent that no real data can be obtained. However, subsequent to that, there appears to be a period when the flow over the projectile is subsonic (at

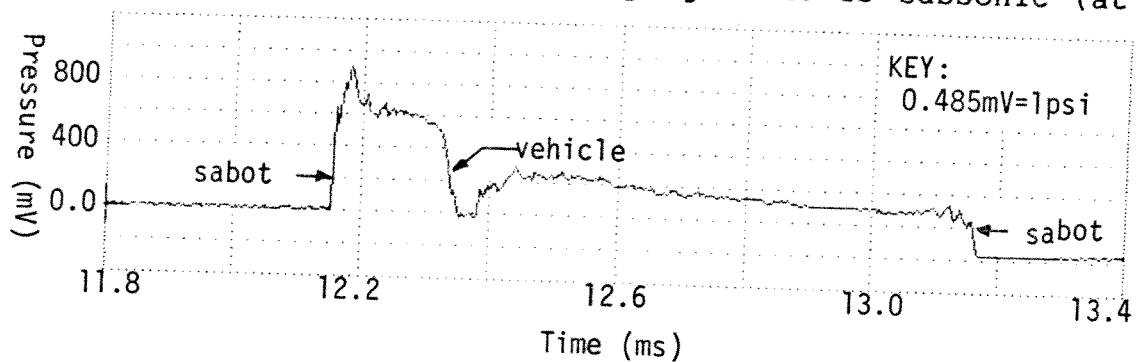


Fig. 16. Pressure vs. Time Output of the Argon Test from Pressure Transducer #3.

transducer #2), and then, as it does in the analysis, the flow chokes at the throat, becomes supersonic, and is followed by another pressure increase before the sabot. This second pressure increase does not, however, appear to be caused by a single shock as the analysis assumes. Rather, it appears to have been caused by a complicated series of shocks. The overall effect appears to be similar, however, to that used in the model. An x-t diagram of the results of this argon test is shown in Fig. 17. Because of the indistinct second shock, its position is not plotted.

For a test of the analysis, the program SABOT was run for 5 atm of argon, using the eventually determined value for the friction drag, the physical properties of argon, and an initial velocity of 1100 m/s. To verify the fact that the flow over the vehicle had started, it was run using condition 1, and then again using condition 1K. Because the sabot shock caught up with the vehicle so quickly, the results were similar, but, as expected, the started case yielded results closer to the actual data. The result of this case is shown on an x-t diagram in Fig. 18.

Because what happens to the vehicle and sabot are what is of primary importance to this thesis, the comparisons between the theoretical and experimental data will be limited to sabot and vehicle characteristics. It is not



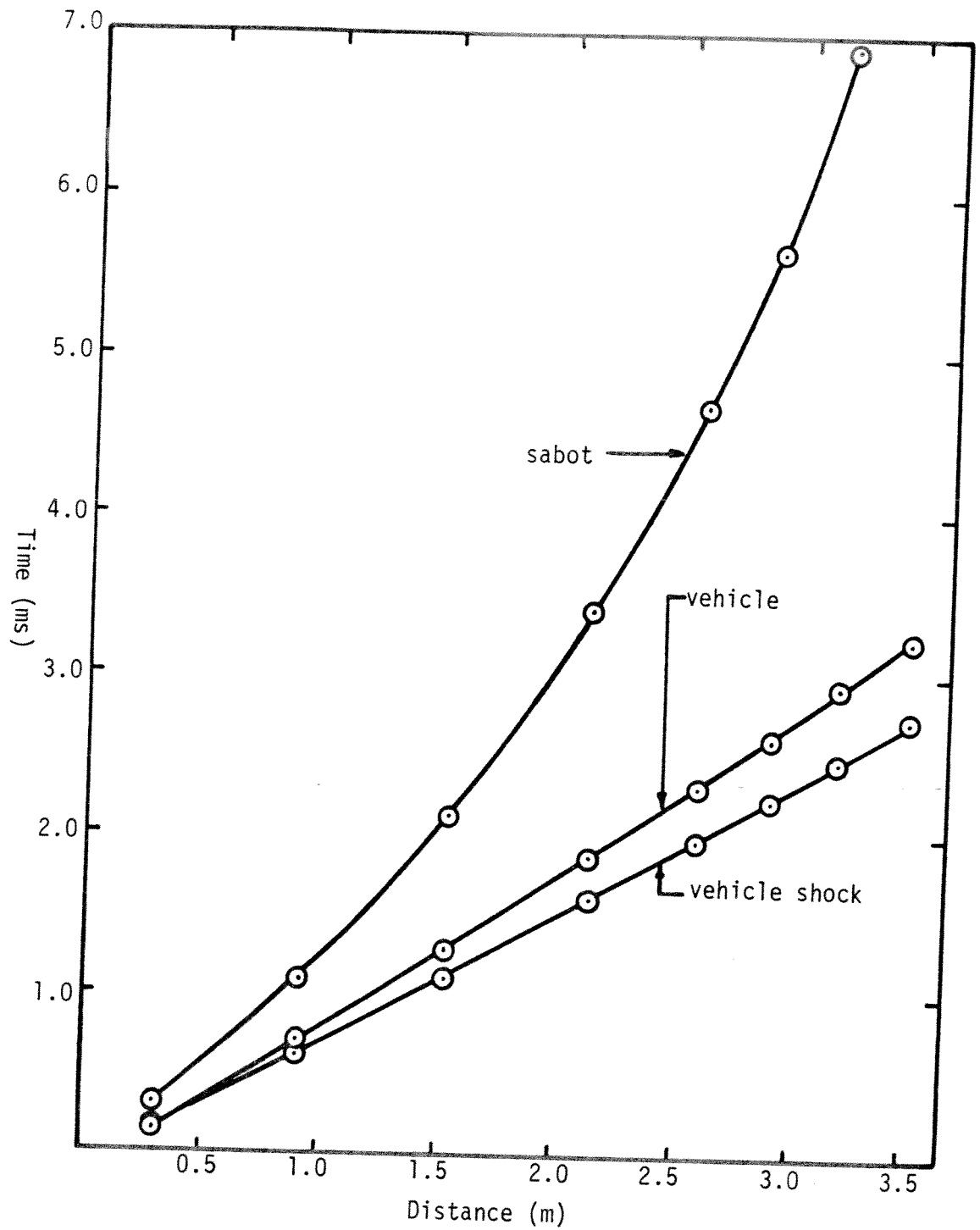


Fig. 17. Plot of Results of Experimental Argon Test.

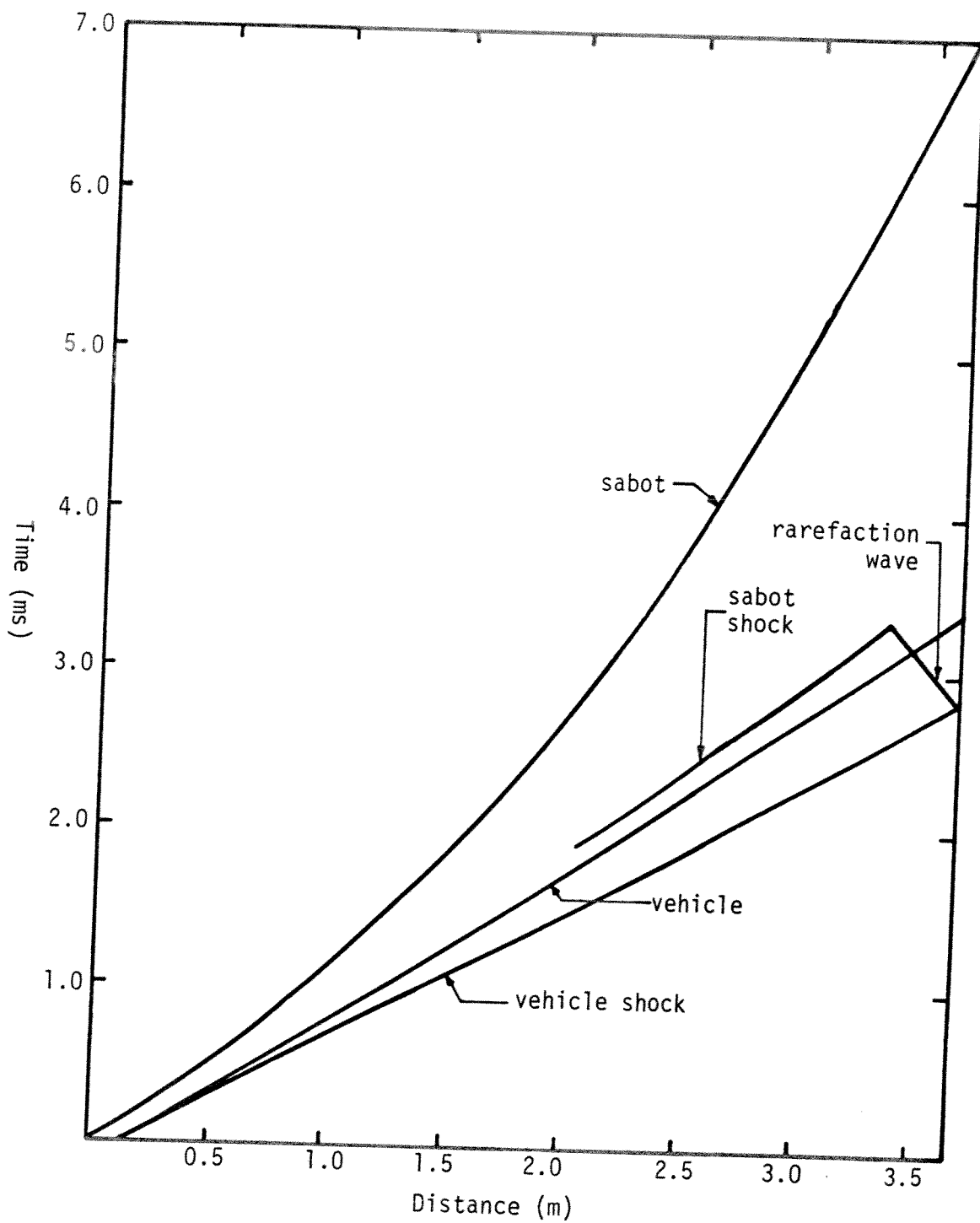


Fig. 18. Plot of Results of Theoretical Argon Test.

very important to have matching shock data, as long as the vehicle and sabot behave similarly in theory and experiment. A comparison of the theoretical and experimental x-t characteristics of the vehicle is shown in Fig. 19. Because the two agree so well, only the last 1-1/2 meters of the tube are represented so a more expanded scale could be used. Despite the expanded scale, because the two curves are so similar, only the theoretical curve is drawn, with the experimental data points being left as is for a comparison. (Due to the fact that the first instrumentation port in the test section is 1.0 ft. down the tube, there is no way of knowing exactly when the experimental vehicle entered the sabot stripper. Therefore, because the vehicle is presumed to slow only very slightly in the first foot of the tube, the positions of the theoretical and experimental vehicles are made to coincide at the first instrumentation port. This assumption is also made in all subsequent x-t diagram comparisons.) In this case, the error is about 1.5%,\* with the theoretical vehicle going faster than the actual one. This accuracy is not unexpected, because most of the approximations in the analysis occur behind the vehicle, and the vehicle spends very little time in condition 5. Also, because friction was ignored, the theoretical vehicle

---

\*The error is defined as the difference between the theoretical and actual exit times divided by the actual exit time.

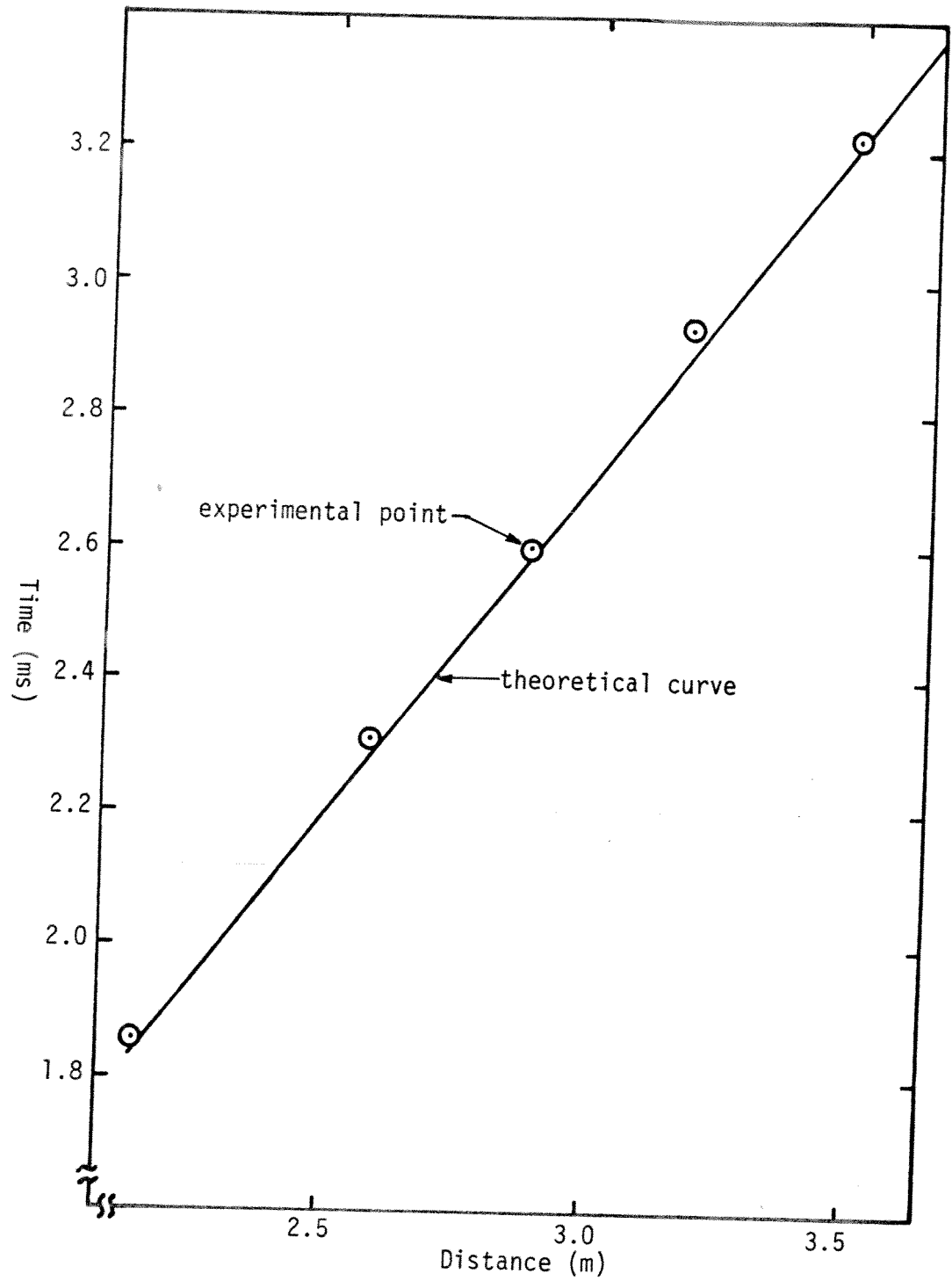


Fig. 19. Comparison of Theoretical and Experimental Characteristics of the Vehicle in Argon.

should be, as it is, too fast. Therefore, the model seems to work quite well for the vehicle in argon. The results show that even the theoretical vehicle's final velocity is approximately 940 m/s, about 6% too slow. Thus, as far as the vehicle is concerned, argon is not satisfactory as a sabot stripping gas.

The comparison between the theoretical and experimental sabot data is shown in Fig. 20. Here, the error is, as expected, much larger, reaching a value at the end of the tube of about 20%. The analysis spends quite a bit of time in conditions 5C and 5D, so much of the error may come from the approximations made in these conditions. A significant error, however, begins to build up early, so the condition 5 analyses are not responsible for all of the errors. Apart from the fact that the flow is not steady, as assumed, some blame must also be put on the assumptions that there would be a single second shock, and that there would be no wake behind the vehicle.

Though this error is relatively large compared to the error in the vehicle calculation, the analysis is still useful. For the most part, the theoretical curve follows a path similar to the experimental curve, and the value of the sabot velocity leaving the tube is higher than the experimentally obtained velocity. Therefore, if the theoretical sabot velocity is slow enough, the experimental value will be slow enough as well. Also, general trends of

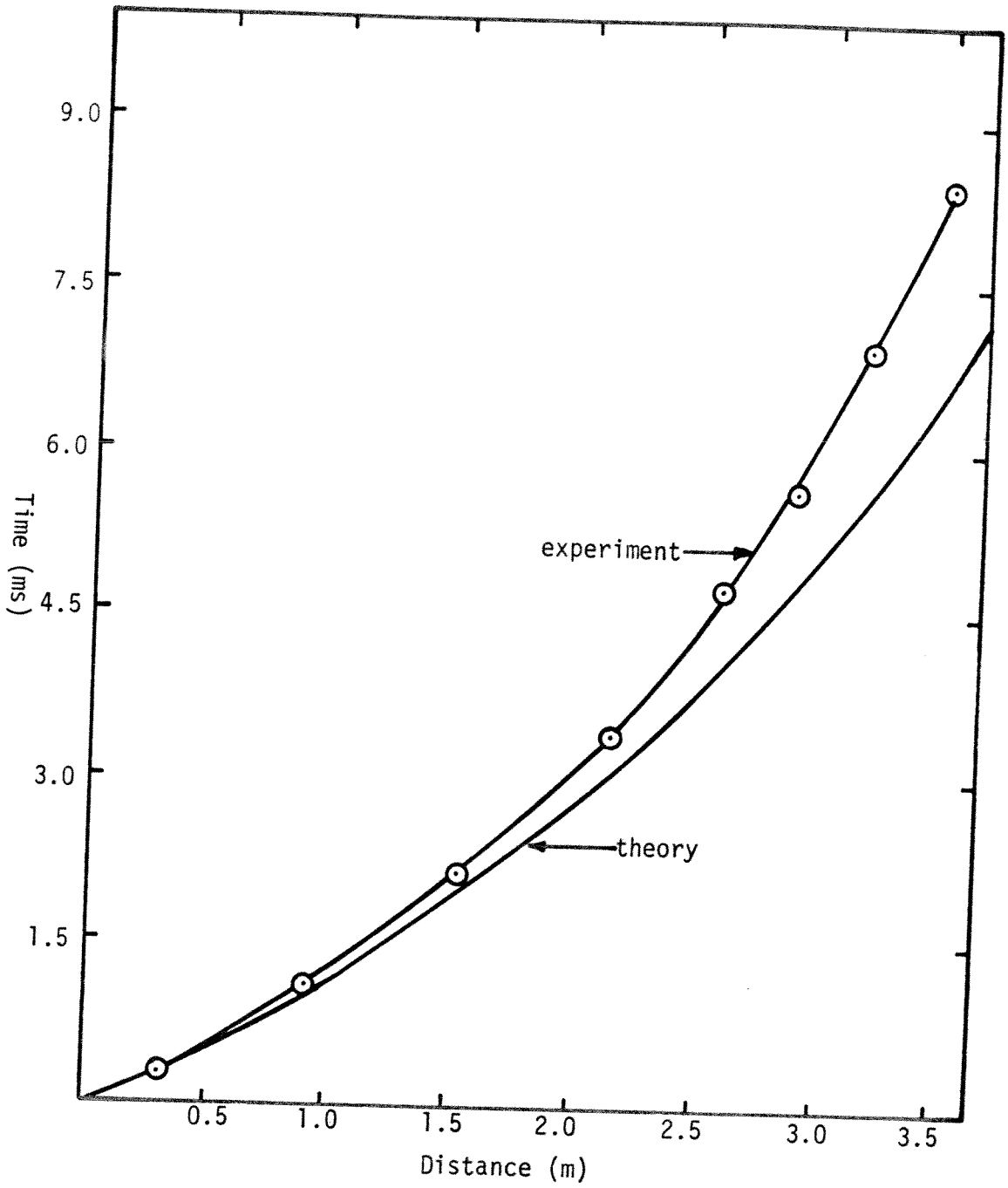


Fig. 20. Comparison of Theoretical and Experimental Characteristics of the Sabot in Argon.

sabot deceleration can be obtained, which are all that was required of the analysis in the first place.

According to the code, the vehicle exits the sabot stripper while the sabot still has 1.33m left to go, and from there, it takes the sabot 3.6 ms to reach the end. Therefore, even if the ram accelerator test section were to be directly after the sabot stripper, the vehicle would be essentially out of the test section before the sabot even entered it. Thus, argon at 5 atm slows the sabot more than adequately, and therefore only fails as a sabot stripping gas because it slows the vehicle too much.

#### Carbon Dioxide Test

Argon is undesirable as a sabot stripping gas because the sabot shock overtook the vehicle, resulting in the flow unstating at the throat formed between the vehicle and the tube wall. This caused the drag on the vehicle to become relatively high, and consequently, the vehicle's final velocity to be too low. To remedy this problem, a gas with a lower ratio of specific heats,  $\gamma$ , and similar molecular weight was selected. If  $\gamma$  is lower, the shock speed for a given condition is slower, so the vehicle has a chance of outrunning the sabot shock and remaining started, and thus remaining fast enough. The readily available gas which meets these criteria is  $\text{CO}_2$ . Accordingly, a test was run with a sabot and vehicle shot into 5 atm of  $\text{CO}_2$ .

Once again, the fiber optic probes at the end of the launch tube were not very useful, except for providing the triggering pulse for the data acquisition system. However, as was hoped, the vehicle started, and remained started throughout the test section. Consequently, the vehicle was readily visible in front of the sabot shock, and an accurate value for its velocity could be obtained. This value was 1096.4 m/s. The positions of the sabot and its shock are also clearly visible. A sample pressure vs. time trace for the CO<sub>2</sub> test showing vehicle, sabot stripper and sabot is shown in Fig. 21. The data from this test are plotted in the form of an x-t diagram in Fig. 22, and all of the outputs from the data acquisition system are displayed in Appendix A.

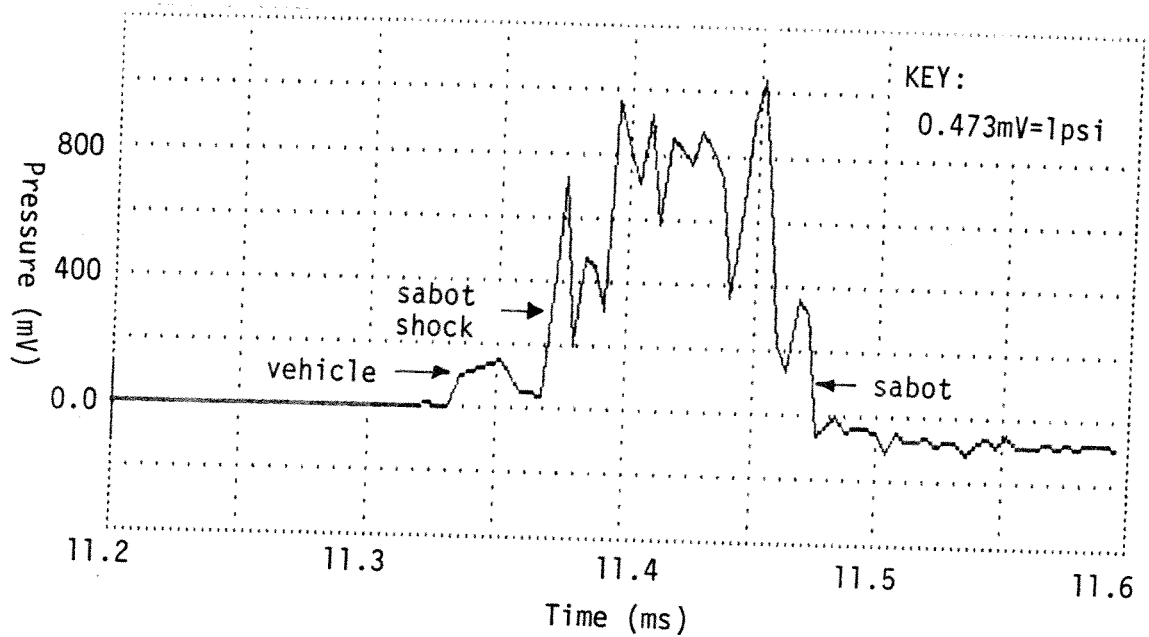


Fig. 21. Pressure vs. Time Output of the CO<sub>2</sub> Test from Pressure Transducer #1.



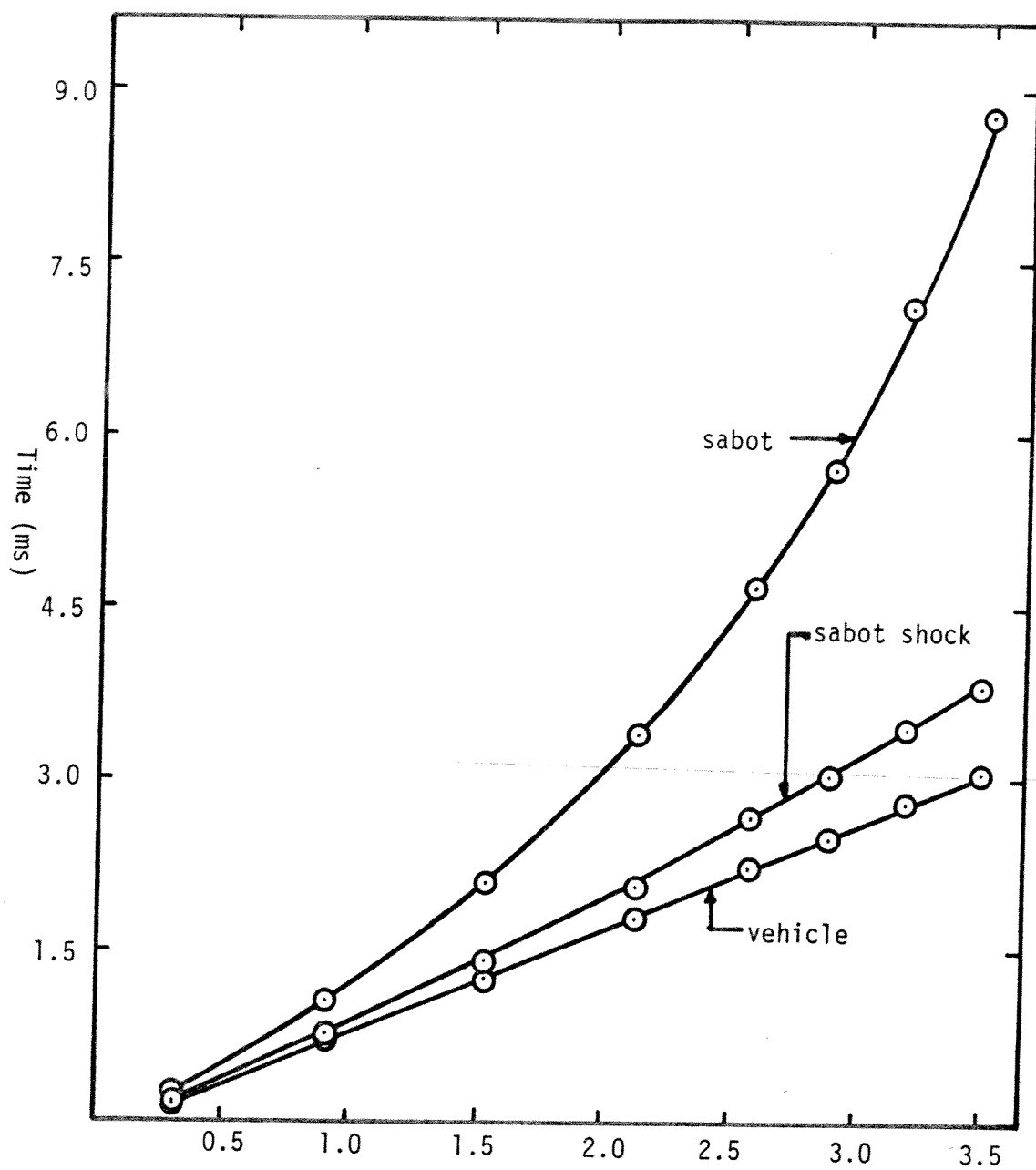


Fig. 22. Plot of Results of Experimental CO<sub>2</sub> Test.

Running the program SABOT for 5 atm of  $\text{CO}_2$  and initial sabot and vehicle velocities of 1100 m/s proved this hypothesis to be correct. An x-t diagram of the results of this run is displayed in Fig. 23. Because the vehicle does not noticeably decelerate in the experimental case, and it cannot decelerate in the theoretical case, the error in the vehicle calculation is essentially zero. Because the vehicle leaves the sabot stripper moving as fast as it came in,  $\text{CO}_2$  is proven to be a good sabot stripping gas, at least as far as the vehicle is concerned.

To determine the merits of  $\text{CO}_2$  from the point of view of sabot deceleration, a comparison of the theoretical and experimental sabot data was made. The results are shown in Fig. 24. The agreement is considerably better than in argon, the error being only about 5%. The error was probably minimized because the most important, early calculations were made in a much simpler flow condition than in the case of the argon. This result also lends some justification to the selection of the value for the friction term.

According to the code, in 5 atm of  $\text{CO}_2$ , the sabot still has 1.5 meters of sabot stripper to travel when the vehicle exits, and it takes 6.3 ms to travel that far, exiting at 160 m/s. This is clearly below the required velocity. Thus,  $\text{CO}_2$  is shown to be an excellent sabot

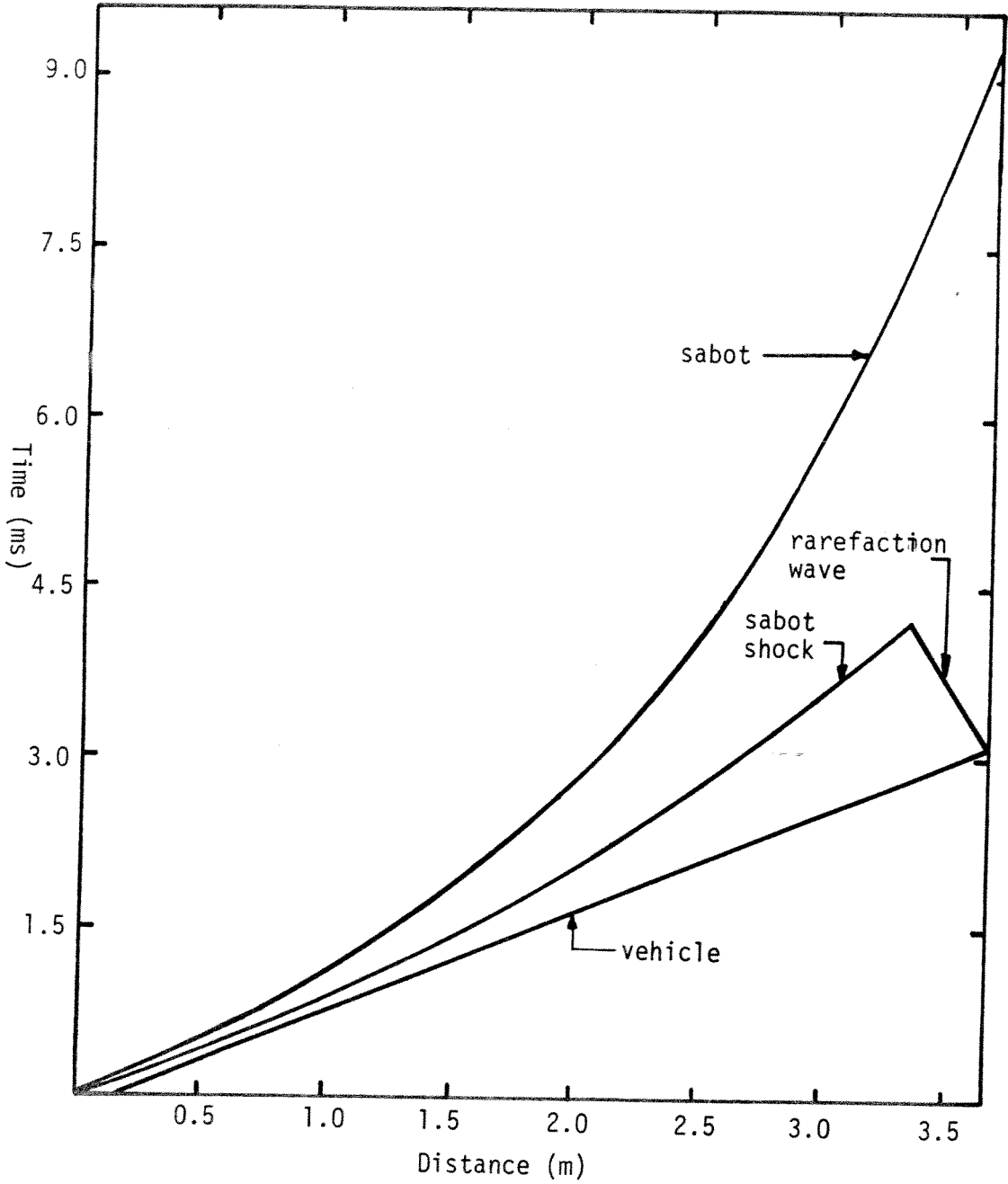


Fig. 23. Plot of Results of Theoretical CO<sub>2</sub> Test.

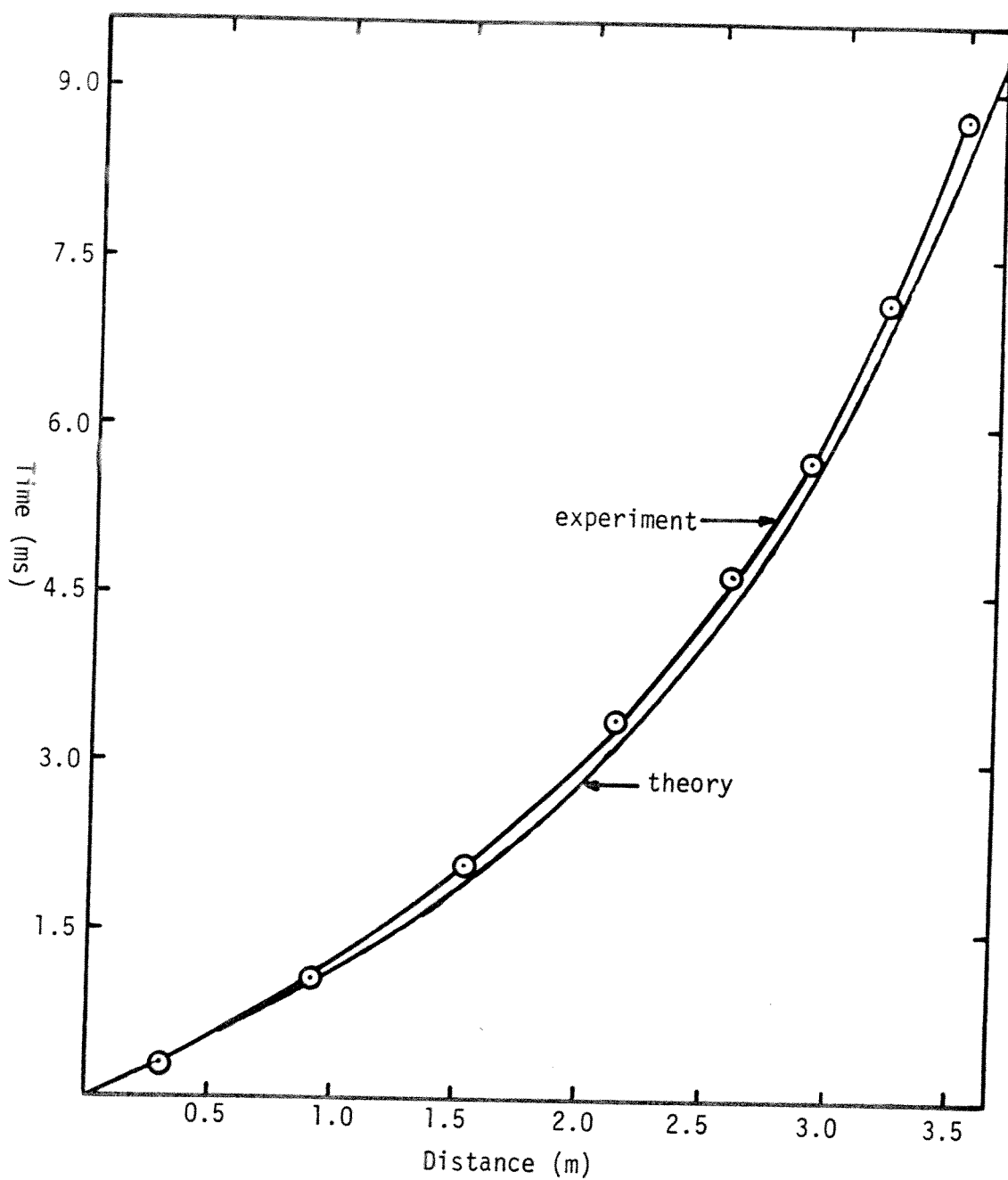


Fig. 24. Comparison of Theoretical and Experimental Characteristics of the Sabot in  $\text{CO}_2$ .

stripping gas in all respects, including reasons not mentioned previously, like cost and availability.

To verify that the experimental data obtained in the two tests described above was valid, spark photographs were taken of the vehicles when they exited the test section. These photographs proved that the vehicles were intact, and that the tests were therefore valid. The photograph of the CO<sub>2</sub> test vehicle is shown in Plate III. Because of technical difficulties, this photograph, though definitely readable, is not very clear. An example of a more successful spark photograph, taken on a subsequent ram accelerator experiment, is shown in Plate IV.

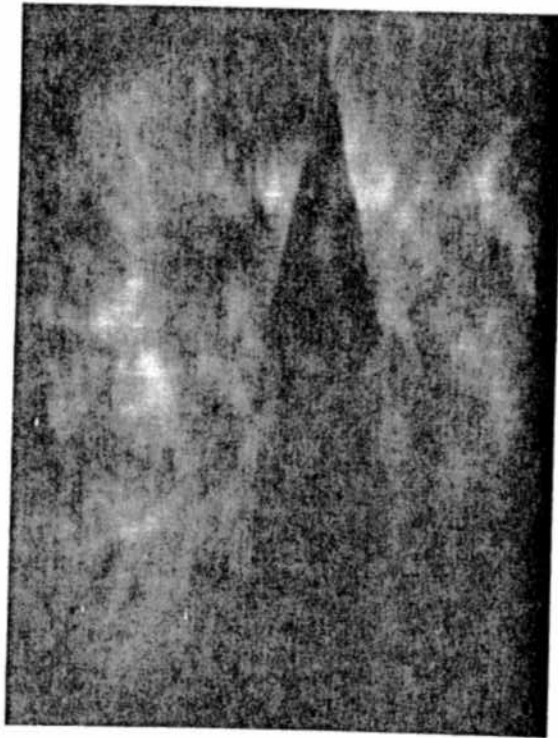


Plate III. Spark Photograph of CO<sub>2</sub> Test Vehicle.

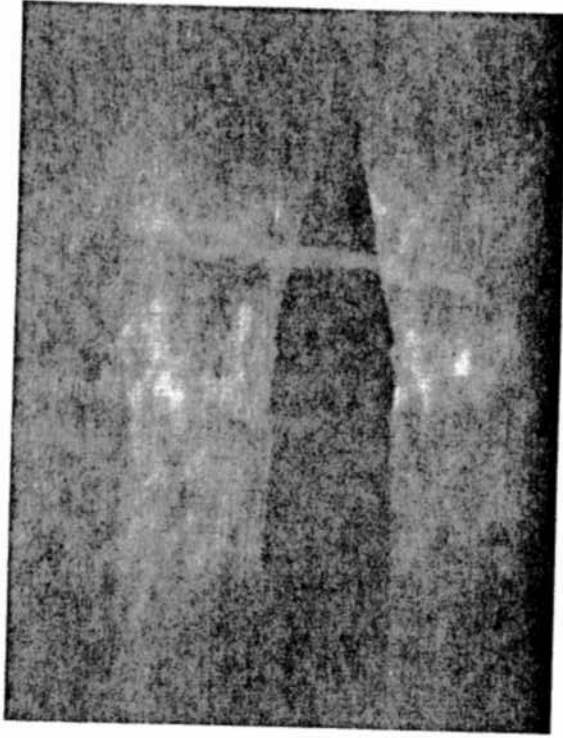


Plate IV. A Clearer Spark Photograph of a Ram Accelerator Vehicle.

## CHAPTER V

### CONCLUSION

Theoretical analyses, backed up by experimental evidence, have shown the feasibility of a useful fluid mechanical sabot stripper. A model of the fluid mechanics within the sabot stripper was developed which, though it implemented approximations for simplicity, yielded results which were accurate enough to be useful. This accuracy was verified by experimental tests.

It was found that argon was not an acceptable gas for the sabot stripper, despite the fact that it slowed the sabot adequately. This is because, in argon, the vehicle was passed by the sabot shock, causing the flow over the vehicle to unstart, increasing the vehicle drag to such an extent that the vehicle velocity became too low. A gas in which this would not happen was sought, and  $\text{CO}_2$  was decided upon.

The sabot shock never caught the vehicle in the theoretical analysis or the experimental test in  $\text{CO}_2$ . This resulted in the vehicle remaining started throughout the entire sabot stripper. Thus, the vehicle drag was minimized, and a usable final vehicle velocity attained.  $\text{CO}_2$  also slowed the sabot more effectively than argon.

The original purpose of this thesis was to find a gas which, when loaded into the sabot stripper, resulted in usable vehicle and sabot velocities.  $\text{CO}_2$  is one such gas. Because  $\text{CO}_2$  is a readily available, safe gas, and because its sabot stripping characteristics are more than adequate, no further gases were investigated.

The results of this thesis will be implemented in the ram accelerator. Also, because the theoretical model developed here has been general, it is hoped that it can continue to be used for analysis of other aspects of the ram accelerator project.



## LIST OF REFERENCES

1. Hertzberg, A., Bruckner, A.P. and Bogdanoff, D.W. "Apparatus and Methods for the Acceleration of Projectiles to Hypervelocities," U.S. Patent Application Serial #623,829, June 22, 1984.
2. Seigel, Arnold E. "The Theory of High Speed Guns," AGARDograph 91, May 1965.
3. Bless, S.J. "Impact Physics Facilities at the University of Dayton Research Institute," in Shock Waves in Condensed Matter-1981, Nellis, W.J., Seaman, L., Graham, R.A., eds., American Institute of Physics Press, New York, 1982.
4. Shapiro, A.H., The Dynamics and Thermodynamics of Compressible Fluid Flow, Vol. 1, John Wiley and Sons, NY, 1953.
5. Timmerhaus, K.D., and Barber, M.S., eds., High Pressure Science and Technology, Vol. 1, Physical Properties and Material Synthesis, and Vol. 2, Applications and Mechanical Properties, Proceedings of Sixth AIRAPT International High Pressure Conference, July 25-29, Plenum Press, New York and London.
6. Kimura, T., Kuwata, C., and Nadai, Y., "Optimum Operating Techniques of Two-Stage Hypersonic Gun Tunnel," p. 1185, AIAA Journal, 16, 11, 1978.

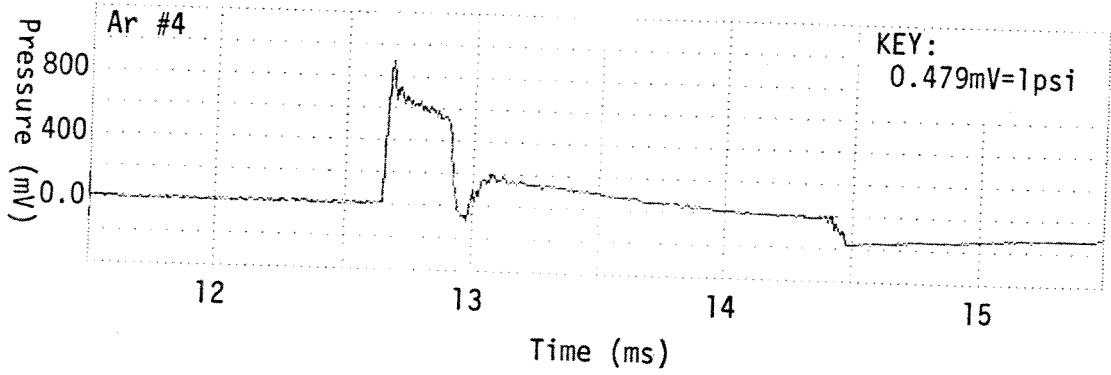
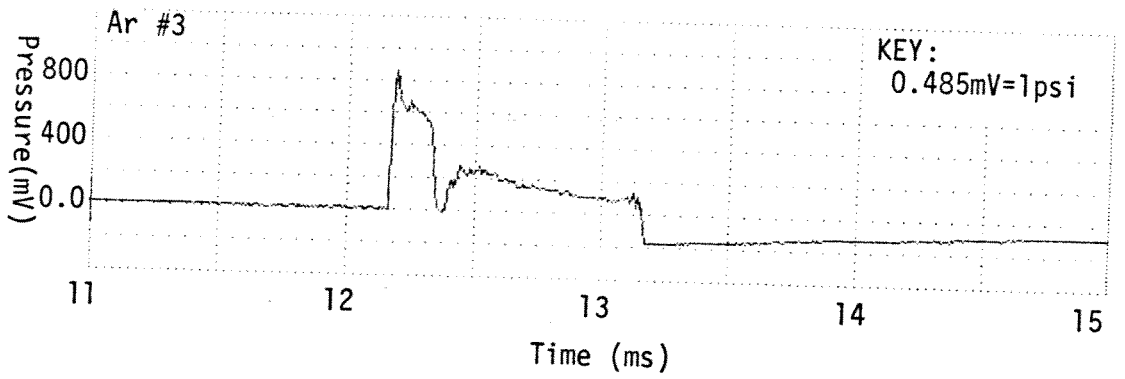
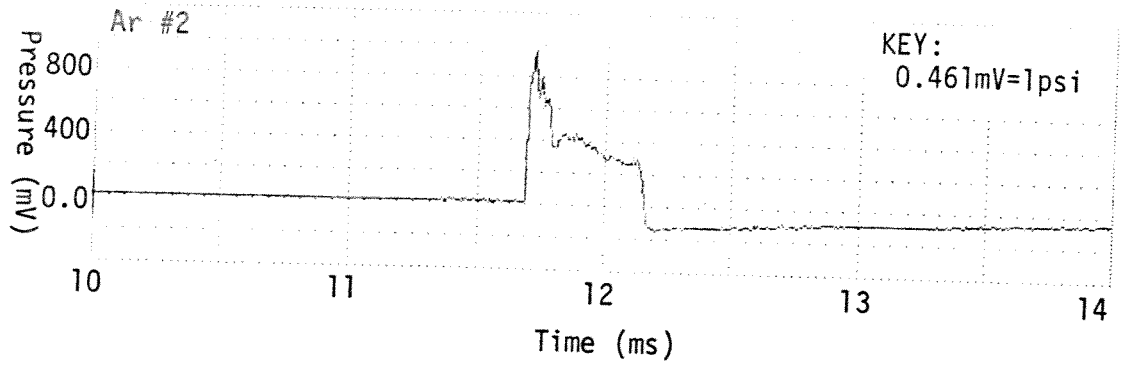
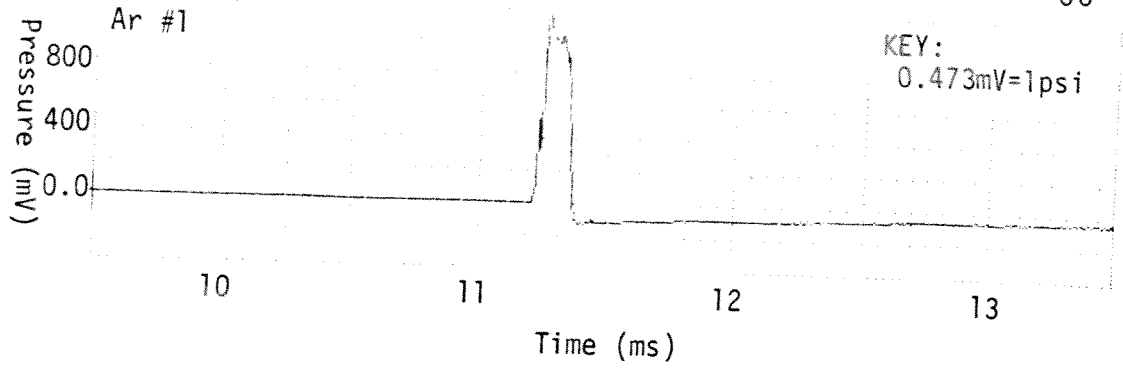
7. Ahrens, T.J., "Dynamic Compression of Earth Materials," Science, 207, 1035, March 1980.

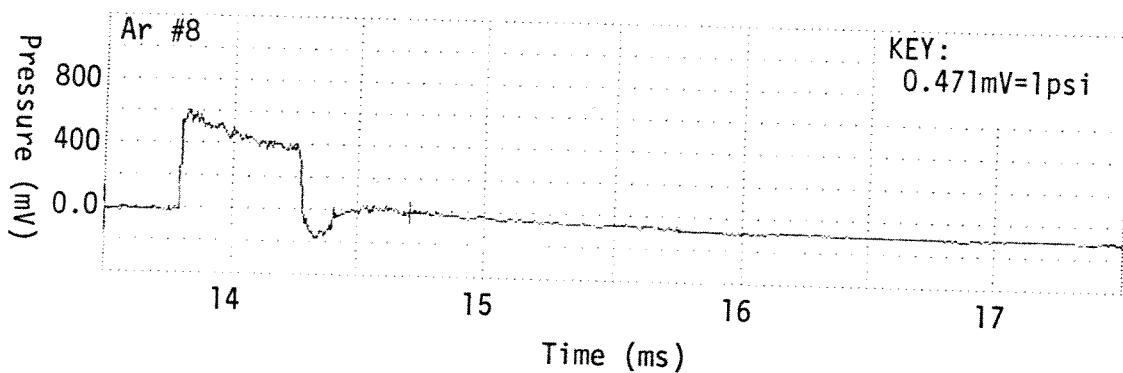
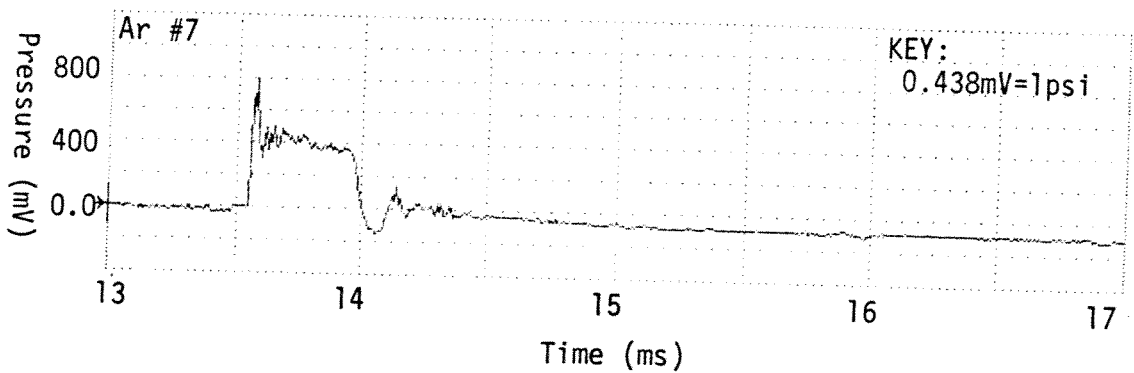
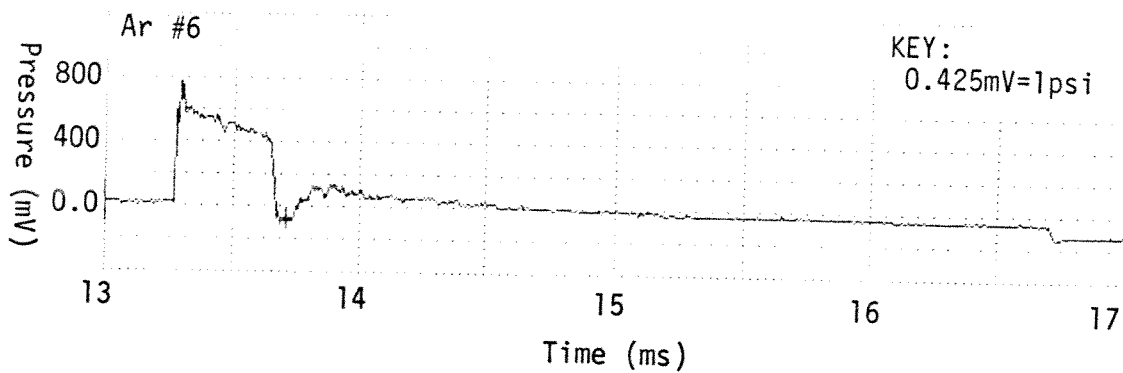
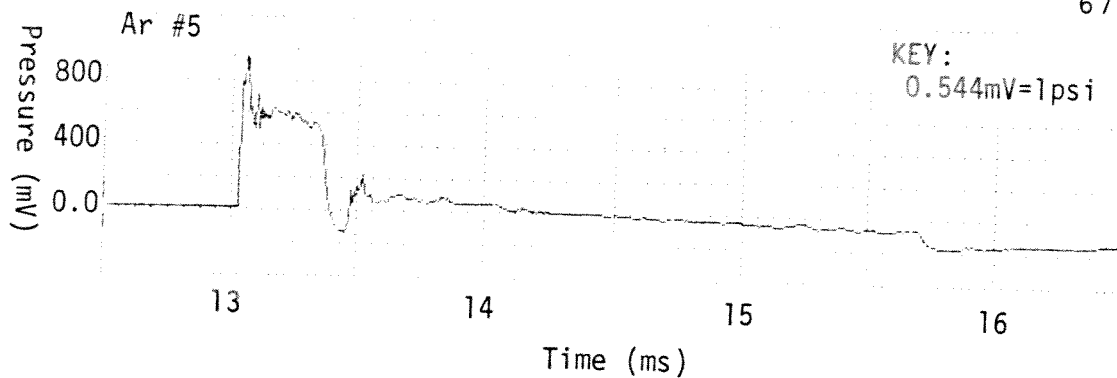
APPENDIX A  
LISTING OF OUTPUT FROM DATA ACQUISITION SYSTEM  
FOR ARGON AND CO<sub>2</sub> TESTS

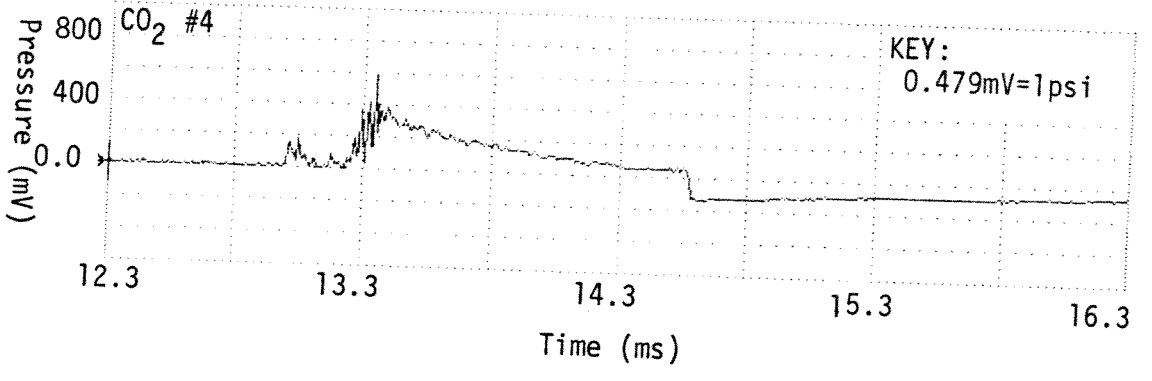
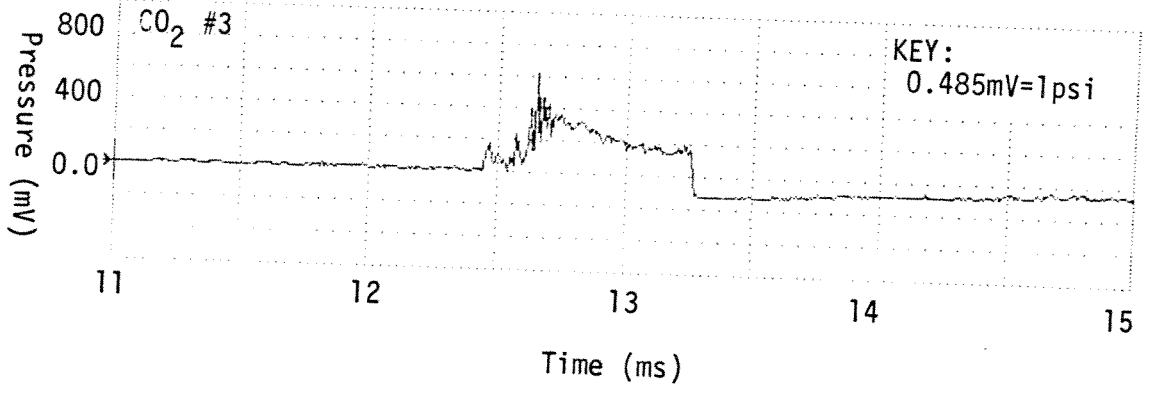
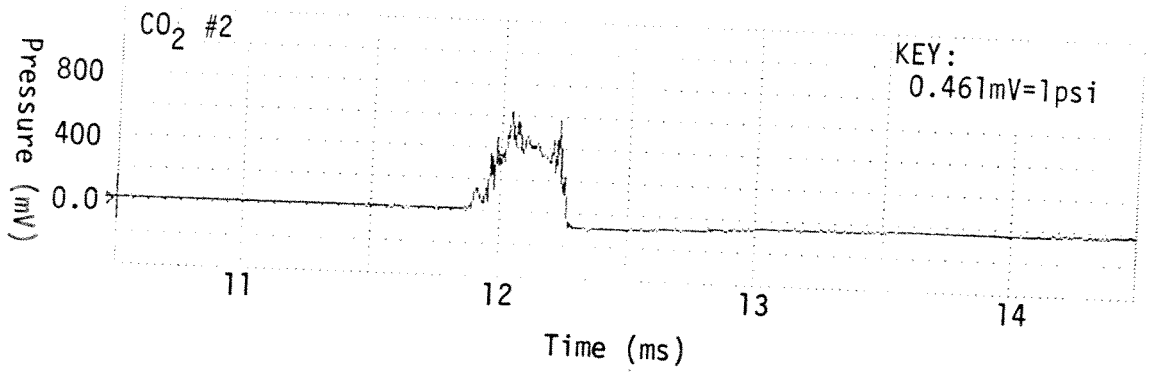
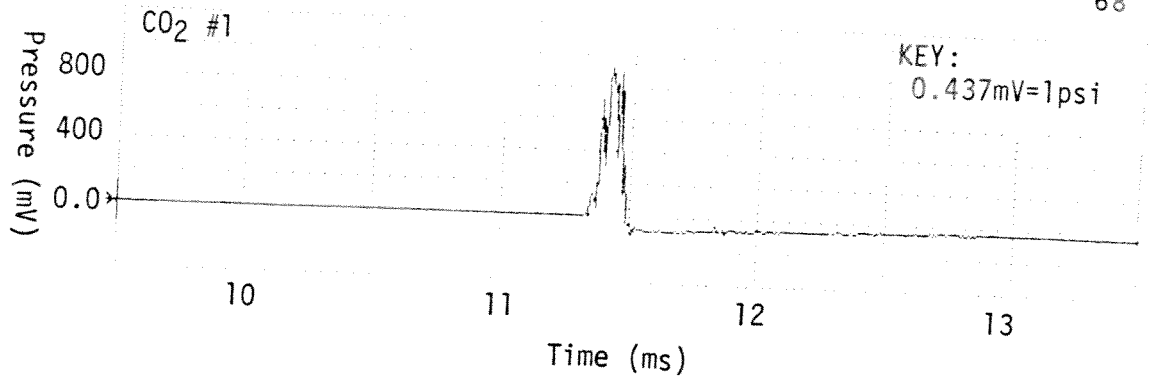
Here follows computer generated output from the two experimental runs. The outputs are in the form of pressure vs. time plots obtained from each Kistler pressure transducer in the test section. The positions of the pressure transducers downstream from the beginning of the test section are given in Table A.1.

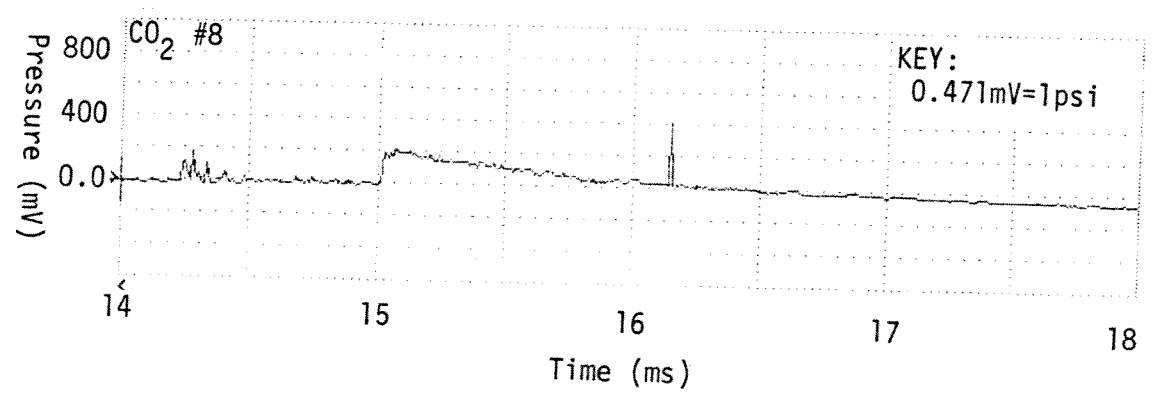
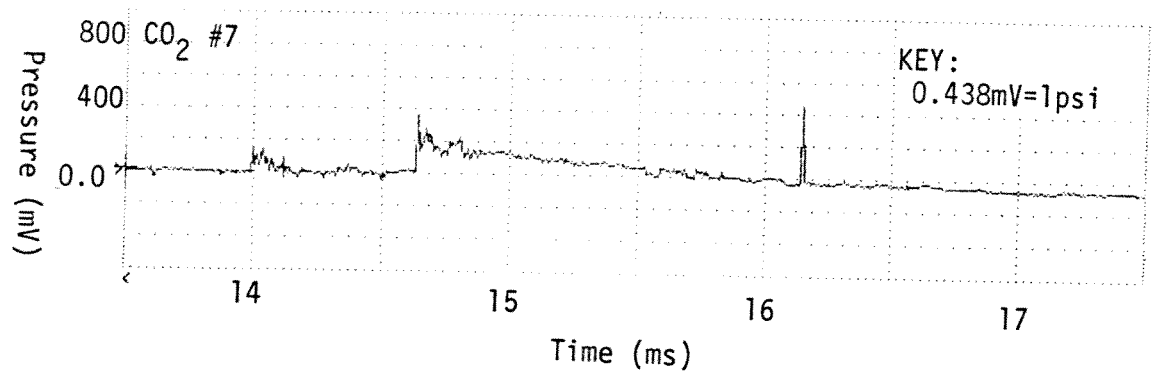
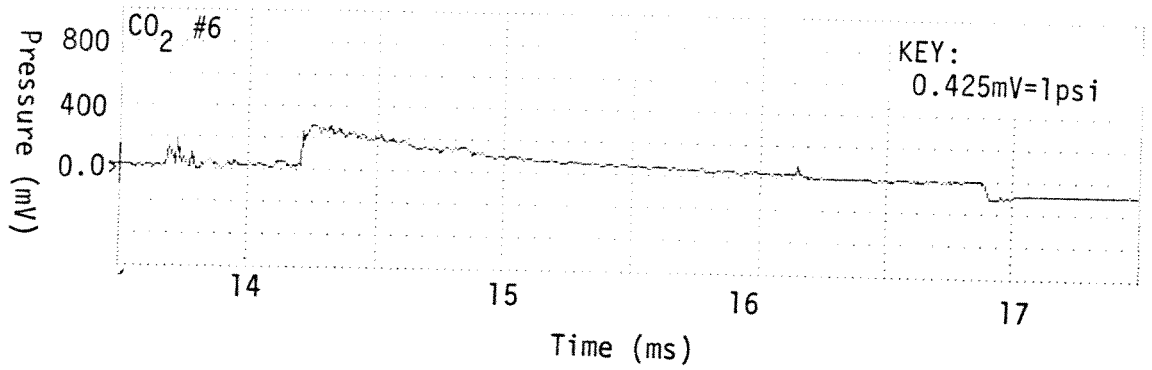
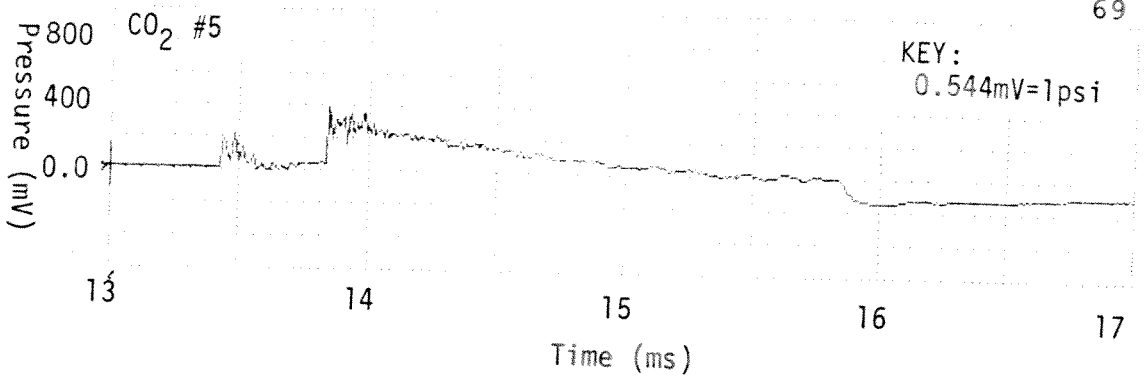
<u>Pressure Transducer #</u>	<u>Position (m)</u>
1	0.3048
2	0.9144
3	1.5240
4	2.1336
5	2.5797
6	2.8845
7	3.1893
8	3.4941

Table A.1. Positions of Pressure Transducers Downstream from the Beginning of the Test Section.









APPENDIX B

LISTING OF FORTRAN PROGRAM SABOT



## PROGRAM SABOT

```

C  * * * * *
C  * THIS PROGRAM CREATES AN APPROXIMATE THEORETICAL *
C  * MODEL TO PREDICT THE INTERACTIONS BETWEEN A *
C  * VEHICLE AND ITS SABOT IN A CLOSED TUBE. *
C  * * * * *
C  *
C  *          VARIABLES OF INTEREST
C  *
C  * APROJ = AREA FOR CALCULATING DRAG ON PROJECTILE *
C  * AR     = AREA RATIO: FLOW AREA OVER THROAT AREA *
C  * ASAB  = CROSS SECTIONAL AREA OF SABOT *
C  * CRITM = SUBSONIC CRITICAL MACH NUMBER *
C  * DP    = PROJECTILE POSITION *
C  * DRAR  = RAREFACTION WAVE POSITION *
C  * DS    = SABOT POSITION *
C  * DSHK1 = FIRST SHOCK POSITION *
C  * DSHK2 = SECOND SHOCK POSITION *
C  * DT    = TIME INCREMENT *
C  * DTH   = THROAT POSITION *
C  * FRICT = FRICTION FACTOR *
C  * GAM   = RATIO OF SPECIFIC HEATS *
C  * P     = PRESSURE *
C  * PL    = PROJECTILE LENGTH *
C  * PROJM = PROJECTILE MASS *
C  * R     = SPECIFIC GAS CONSTANT *
C  * RHO   = MASS DENSITY *
C  * SABM  = SABOT MASS *
C  * SCRITM= SUPERSONIC CRITICAL MACH NUMBER *
C  * SS    = SOUND SPEED *
C  * T     = TEMPERATURE *
C  * TL    = TUBE LENGTH *
C  * UPROJ = PROJECTILE VELOCITY *
C  * URAR  = RAREFACTION WAVE VELOCITY *
C  * USAB  = SABOT VELOCITY *
C  *
C  * NUMBERS FOLLOWING VARIABLE NAMES (E.G.T1) *
C  * REFER TO THAT VARIABLE AT A LOCATION IN THE *
C  * FLOW. USUALLY, 1 REFERS TO INITIAL CONDITIONS, *
C  * 2 TO AFTER THE FIRST SHOCK, 3 TO THE NOSE *
C  * OF THE PROJECTILE, ETC. *
C  *
C  * ALL OTHER VARIABLES CAN BE DETERMINED FROM *
C  * THE ABOVE. *
C  *
C  * ALL ITERATION USES THE METHOD OF HALVING, AND *
C  * IS DONE TO 0.1%. *
C  * * * * *

```

```

COMMON/A/GAM, GM1, GP1
COMMON/B/USABR, USABL, SS2G, ZM1G, ZM2G, USABG
COMMON/C/ARR, ARL, SMR, SML, ARG, SMG

```

```

COMMON/D/SS1,ZMFR,ZMFL,QM1R,QM1L,QM1G,QM2G,ZMF,
$   CRITM
COMMON/E/SCRITM
COMMON/F/AR
COMMON/G/T,DS,DP
COMMON/H/USAB,UPROJ
COMMON/I/DT
COMMON/J/AVE
DATA T1,P1,RHO1,GAM,R/298.,506625.,8.168,1.667,208.13/
DATA SABM,PROJM,USAB,AR,TL,DT/.037,.072,1100.,2.38552,
$   3.657,1.E-4/
FRICT=750.0
PL=0.1468
PI=3.14159
ASAB=PI*(.01905**2.0)
APROJ=ASAB
UPROJ=USAB
OLDV=UPROJ
DTH=0.07676
DP=PL
DS=0.0
DSHK1=0.0
DSHK2=0.0
PUSHK1=0.0
PUSHK2=0.0
GM1=GAM-1.0
GP1=GAM+1.0
SS1=SQRT(GAM*R*T1)
K=1

```

```

C
C   IF K=1, THE VEHICLE IS ASSUMED STARTED INITIALLY.
C   ANY OTHER VALUE ASSUMES A KANTROWICZ UNSTART.
C

```

```

IND=2

```

```

C
C   CALCULATE CRITM AND SCRITM FROM AREA RATIO BY
C   ITERATION. NOTE: ONLY GOOD FOR GAMMA = 1.1 -->
C   2.0
C

```

```

SML=0.237
SMR=0.261
10  ARL=CAR(SML)
ARR=CAR(SMR)
20  CALL ALGMC
IF ((ABS(ARG-AR)).LT.(AR*.001)) GOTO 40
IF (ARG.GT.AR) GOTO 30
SMR=SMG
ARR=ARG
GOTO 20
30  SML=SMG
ARL=ARG

```

```

GOTO 20
40  IF (N.EQ.1) GOTO 50
    CRITM=SMG
    PRINT*, 'CRITM= ', CRITM
    SML=2.12
    SMR=3.04
    N=1
    GOTO 10
50  SCRITM=SMG
    PRINT*, 'SCRITM= ', SCRITM
    PRINT*, 'FRICT=', FRICT

C
C  * * * * *
C  *                               CONDITION 1K
C  * * * * *
C  *                               VEHICLE ASSUMED UNSTARTED
C  * * * * *
C
C  ITERATION TO FIND FIRST SHOCK STRENGTH (QM1G)
C  BASED ON CRITM AT PROJECTILE NOSE.
C
    IF (K.EQ.1) GOTO 145
    IND=0
    DSHK1=PL
    QM1R=5.0
    QM2R=CM2(QM1R)
    QSS2R=SS1*CA2PA1(QM1R, QM2R)
    U1R=QM1R*SS1
    U2R=QM2R*QSS2R
    U2PR=U1R-U2R
    ZMFR=(UPROJ-U2PR)/QSS2R
60  QM1L=1.0
    U2PL=0.0
    ZMFL=(UPROJ-U2PL)/SS1
70  CALL ALGST
    IF ((ABS(ZMF-CRITM)).LT.(CRITM*.001)) GOTO 90
    IF (ZMF.GT.CRITM) GOTO 80
    QM1R=QM1G
    ZMFR=ZMF
    GOTO 70
80  QM1L=QM1G
    ZMFL=ZMF
    GOTO 70
90  USHK1=QM1G*SS1
    IF (PUSHK1.EQ.0.0)GOTO 100
    CALL SUSHK(USHK1, PUSHK1, DDSHK1)
    AVE1=AVE
    DSHK1=DSHK1+DDSHK1
    PRINT*, 'AT T= ', T, 'DSHK1= ', DSHK1
    GOTO 105
100 PUSHK1=USHK1

```

```

105  SS2=SS1*CA2PA1(QM1G,QM2G)
      SST3=SS2*CTSS2(CRITM)
      P2=P1*CP2(QM1G,QM2G)
      PT3=P2*CTP2(CRITM)
      RH02=RH01*CP2(QM1G,QM2G)/((CA2PA1(QM1G,QM2G)**2.0)
      RH0T3=RH02*CTRH02(CRITM)
110  SS4=SST3/CTSS2(SCRITM)
      PRINT*, 'K-1'
      U4=SCRITM*SS4
      UREL=U4-UPROJ

C
C  ITERATION TO DETERMINE SECOND SHOCK STRENGTH (ZM5G)
C
      ZM5R=5.0
      ZM6R=CM2(ZM5R)
      U5R=ZM5R*SS4
      SS6R=SS4*CA2PA1(ZM5R,ZM6R)
      U6R=ZM6R*SS6R
      USHKR=U5R-UREL
      USABR=USHKR-U6R
      ZM5L=1.0
      USABL=-UREL
120  TSLOPE=(USABR-USABL)/(ZM5R-ZM5L)
      TYO=USABL-(ZM5L*TSLOPE)
      ZM5G=(USABR-TYO)/TSLOPE
      U5G=ZM5G*SS4
      ZM6G=CM2(ZM5G)
      SS6G=SS4*CA2PA1(ZM5G,ZM6G)
      U6G=ZM6G*SS6G
      USHKG=U5G-UREL
      USABG=USHKG-U6G
      IF((ABS(USABG-USAB)).LT.(USAB*.001))GOTO 130
      IF(USABG.GT.USAB)GOTO 125
      ZM5L=ZM5G
      USABL=USABG
      GOTO 120
125  ZM5R=ZM5G
      USABR=USABG
      GOTO 120
130  USHK2=USHKG
      IF(PUSHK2.EQ.0.0)GOTO 135
      CALL SUSHK(USHK2,PUSHK2,DDSHK2)
      DDSHK2=DSHK2+DDSHK2

C
C  IF SHOCK CATCHES THROAT, ANALYSIS GOES TO CONDITION
C  2.
C
      IF(DSHK2.GE.(DP-DTH)) GOTO 142
      PRINT*, 'AT T= ',T,'DSHK2= ',DSHK2
      GOTO 140
135  DSHK2=DP-PL

```

PUSHK2=USHK2

C  
C  
C

IF SHOCK EXITS TUBE, ANALYSIS GOES TO CONDITION 5

140

IF (DSHK1.GT.TL)GOTO 700  
P4=PT3/CTP2(SCRITM)  
RHO4=RHOT3/CTRHO2(SCRITM)  
P6=P4\*CP2(ZM5G,ZM6G)  
RHO6=RHO4\*CP2(ZM5G,ZM6G)/(CA2PA1(ZM5G,ZM6G)\*\*2.)  
FSAB=P6\*ASAB+FRICT  
DDS=(.5\*(-FSAB/SABM)\*(DT\*\*2.))+(USAB\*DT)  
USAB=USAB-((FSAB/SABM)\*DT)

C  
C  
C

IF SABOT STOPS, ANALYSIS TERMINATES

IF (USAB.LT.0.0)GOTO 800  
U3=CRITM\*SS2  
U4=SCRITM\*SS4  
FPROJ=((P2+(RHO2\*(U3\*\*2.)))-(P4+(RHO4\*U4\*\*2.)))  
\$ \*APROJ  
DDP=(.5\*(-FPROJ/PROJM)\*(DT\*\*2.))+(UPROJ\*DT)  
OLDV=UPROJ  
UPROJ=UPROJ-((FPROJ/PROJM)\*DT)  
T=T+DT  
DS=DDS+DS  
DP=DDP+DP  
CALL PDAT  
SSE2=SS2  
QM1R=QM1G  
QSS2G=SS1\*CA2PA1(QM1G,QM2G)  
U1G+QM1G\*SS1  
U2G=QM2G\*QSS2G  
U2PG=U1G-U2G  
ZMFR=(UPROJ-U2PG)/QSS2G  
GOTO 60

142

PUSHK2=0.0  
USHK2=0.0  
PUSHK1=0.0  
DSHK2=0.0  
GOTO 198

C  
C  
C  
C  
C  
C  
C

\* \* \* \* \*  
\*  
\* \* \* \* \* CONDITION 1 \*  
\* \* \* \* \*  
\* VEHICLE ASSUMED STARTED UPON ENTRY INTO TUBE \*

ITERATION TO FIND SABOT SHOCK STRENGTH (ZM1G)

145

ZM1R=5.0  
U1R=ZM1R\*SS1  
ZM2R=CM2(ZM1R)  
SS2R=SS1\*CA2PA1(ZM1R,ZM2R)

```

      U2R=ZM2R*SS2R
      USABR=U1R-U2R
150   ZM1L=1.5
      U1L=ZM1L*SS1
      ZM2L=CM2(ZM1L)
      SS2L=SS1*CA2PA1(ZM1L,ZM2L)
      U2L=ZM2L*SS2L
      USABL=U1L-U2L
160   CALL ALGOI(SS1,ZM1L,ZM1R)
      IF((ABS(USABG-USAB)).LT.(USAB*.001))GO TO 180
      IF(USABG.GT.USAB) GOTO 170
      ZM1L=ZM1G
      USABL=USABG
      GOTO 160
170   ZM1R=ZM1G
      USABR=USABG
      GOTO 160
180   PRINT*,'ZERO'
      USHK1=ZM1G*SS1
      IF(PUSHK1.EQ.0.0)GOTO 185
      CALL SUSHK(USHK1,PUSHK1,DDSHK1)
      AVE1=AVE
      DSHK1=DSHK1+DDSHK1

C
C   IF SHOCK CATCHES UP WITH SHOCK, ANALYSIS MOVES TO
C   CONDITION 2
C
      IF(DSHK1.GE.(DP-DTH)) GOTO 195
      PRINT*,'AT T= ',T,'DSHK1= ',DSHK1
      GOTO 190
185   PUSHK1=USHK1
190   P2=P1*CP2(ZM1G,ZM2G)
      FSAB=(P2*ASAB)+FRICT
      DDS=(.5*(-FSAB/SABM)*(DT**2))+(USAB*DT)
      USAB=USAB-((FSAB/SABM)*DT)
      IF(USAB.LT.0.0)GOTO 800
      DDP=UPROJ*DT
      T=T+DT
      DS=DS+DDS
      DP=DP+DDP
      CALL PDAT

C
C   IF VEHICLE EXITS TUBE, ANALYSIS MOVES TO CONDITION
C   5C
C
      IF (DP.GT.TL) GOTO 767
      SS2E=SS2G
192   ZM1R=ZM1G
      USABR=USABG
      GOTO 150
195   DSHK1=DP

```

```

PUSHK1=0.0
PRINT*.'AT T= ',T,'DSHK1= ',DSHK1
GOTO 230
C   * * * * *
C   *
C   * * * * *          CONDITION 2
C   * * * * *          * * * * *
C   * SHOCK IN FRONT OF VEHICLE, FLOW EVERYWHERE
C   * SUBSONIC OVER VEHICLE
C   * * * * *
C
C   ITERATION TO FIND SHOCK STRENGTH (ZM1G)
C
198  ZM1R=5.0
    U1R=ZM1R*SS1
    ZM2R=CM2(ZM1R)
    SS2R=SS1*CA2PA1(ZM1R,ZM2R)
    U2R=ZM2R*SS2R
    USABR=U1R-U2R
200  ZM1L=1.5
    U1L=ZM1L*SS1
    ZM2L=CM2(ZM1L)
    SS2L=SS1*CA2PA1(ZM1L,ZM2L)
    U2L=ZM2L*SS2L
    USABL=U1L-U2L
210  CALL ALGO1(SS1,ZM1L,ZM1R)
    IF((ABS(USABG-USAB)).LT.(USAB*.001)) GO TO 230
    IF(USABG.GT.USAB) GOTO 220
    ZM1L=ZM1G
    USABL=USABG
    GOTO 210
220  ZM1R=ZM1G
    USABR=USABG
    GOTO 210
C
C   WHEN FLOW CHOKES, ANALYSIS GOES TO CONDITION 3
C
230  ZMFLOW=(UPROJ-USAB)/SS2G
    IF (ZMFLOW.GE.CRITM) GOTO 300
    PRINT*, 'ONE'
    IND=2
    USHK1=ZM1G*SS1
    IF(PUSHK1.EQ.0.0) GOTO 240
    CALL SUSHK(USHK1,PUSHK1,DDSHK1)
    DSHK1=DSHK1+DDSHK1
    PRINT*,'AT T= ',T,'DSHK1= ',DSHK1
    IF (DSHK1.GT.TL)GOTO 700
    GOTO 250
240  PUSHK1=USHK1
250  P2=P1*CP2(ZM1G,ZM2G)
    FSAB=(P2*ASAB)+FRICT
    DDS=(.5*(-FSAB/SABM)*(DT**2))+(USAB*DT)

```

```

USAB=USAB-((FSAB/SABM)*DT)
IF(USAB.LT.0.0)GOTO 800
DDP=UPROJ*DT
T=T+DT
DS=DS+DDS
DP=DP+DDP
CALL PDAT
SS2E=SS2G
ZM1R=ZM1G
USABR=USABG
GOTO 200
C * * * * *
C *
C * * * * *          CONDITION 3
C * * * * *          *
C * FLOW CHOKED AT THROAT, SECOND SHOCK ON VEHICLE *
C * * * * *          *
C
C ITERATION TO FIND FIRST SHOCK STRENGTH (QM1G)
C
300 QM1R=5.0
    QM2R=CM2(QM1R)
    QU1R=QM1R*SS1
    QSS2=SS1*CA2PA1(QM1R,QM2R)
    QU2R=QM2R*QSS2
    QU2PR=QU1R-QU2R
    ZMFR=(UPROJ-QU2PR)/QSS2
310 QM1L=1.0
    U2PL=0.0
    ZMFL=(UPROJ-U2PL)/SS1
320 CALL ALGST
    IF ((ABS(ZMF-CRITM)).LT.(CRITM*.001)) GOTO 340
    IF (ZMF.GT.CRITM) GOTO 330
    QM1R=QM1G
    ZMFR=ZMF
    GOTO 320
330 QM1L=QM1G
    ZMFL=ZMF
    GOTO 320
340 USHK1=QM1G*SS1
    IF(PUSHK1.EQ.0.0)GOTO 350
    CALL SUSHK(USHK1,PUSHK1,DDSHK1)
    AVE1=AVE
    DSHK1=DSHK1+DDSHK1
    PRINT*, 'AT T= ',T, 'DSHK1= ',DSHK1
    IF (DSHK1.GT.TL)GOTO 700
    GOTO 360
350 PUSHK1=USHK1
360 SS2=SS1*CA2PA1(QM1G,QM2G)
    PRINT*, 'TWO'
    IND=1
    SST3=SS2*CTSS2(CRITM)

```



```

P2=P1*CP2(QM1G,QM2G)
PT3=P2*CTP2(CRITM)
RHO2=RHO1*CP2(QM1G,QM2G)/(CA2PA1(QM1G,QM2G)**2.0)
RHOT3=RHO2*CTRH02(CRITM)
C
C
C
CHECK IF ASH/A*>AR.  IF SO, GOTO CONDITION 4

EM2=CM2(SCRITM)
ESS4=SST3*(1.0/CTSS2(SCRITM))
ESS5=ESS4*CA2PA1(SCRITM,EM2)
EU2=EM2*ESS5
EUSAB=UPROJ-EU2
IF(EUSAB.GE.USAB) GOTO 540
C
C
C
ITERATE TO FIND AREA RATIO AT SECOND SHOCK (GAR)

GARL=1.0
GM6L=CRITM
GARR=AR
GM6R=EM2
400 SS6L=SST3/CTSS2(GM6L)
SS6R=SST3/CTSS2(GM6R)
U6L=GM6L*SS6L
U6R=GM6R*SS6R
GUSABL=UPROJ-U6L
GUSABR=UPROJ-U6R
SLOPE=(GUSABR-GUSABL)/(GARR-GARL)
YO=GUSABL-(GARL*SLOPE)
GAR=(USAB-YO)/SLOPE
L=0
CALL ZITAR(GAR,GGM4,L)
GGM5=CM2(GGM4)
GIAR=CAR(GGM5)
ZAR=AR*GIAR/GAR
L=2
CALL ZITAR(ZAR,ZZM6,L)
SSZZ6=SST3/CTSS2(ZZM6)
UZZ6=ZZM6*SSZZ6
ZZUSAB=UPROJ-UZZ6
C
C
C
ZZUSAB=USAB CORRESPONDING TO GAR

IF ((ABS(ZZUSAB-USAB)).LT.(.001*USAB))GOTO 420
IF (ZZUSAB.GT.USAB) GOTO 410
GARR=GAR
GM6R=ZZM6
GOTO 400
410 GARL=GAR
GM6L=ZZM6
GOTO 400
420 PT5=PT3*CP2(GGM4,GGM5)*CTP2(GGM5)/CTP2(GGM4)

```

```

P6=PT5/CTP2(ZZM6)
RHOT5=RHOT3*CP2(GGM4,GGM5)*CTRH02(GGM5)/((CA2PA1
$ (GGM4,GGM5)**2.)*CTRH02(GGM4))
RHO6=RHOT5/CTRH02(ZZM6)
FSAB=(P6*ASAB)+FRICT
DDS=(.5*(-FSAB/SABM)*(DT**2.))+ (USAB*DT)
USAB=USAB-((FSAB/SABM)*DT)
IF (USAB.LT.0.0)GOTO 800
U3=CRITM*SS2
U6=UZZ6
FPROJ=((P2+(RHO2*U3**2.))- (P6+RHO6*(U6**2.)))*
$ APROJ
DDP=(.5*(-FPROJ/PROJM)*(DT**2.))+ (UPROJ*DT)
OLDV=UPROJ
UPROJ=UPROJ-((FPROJ/PROJM)*DT)
T=T+DT
DS=DS+DDS
DP=DP+DDP
CALL PDAT
SSE2=SS2
Q1R=Q1G
QSS2G=SS1*CA2PA1(QM1G,QM2G)
U1G=QM1G*SS1
U2G=QM2G*QSS2G
U2PG=U1G-U2G
ZMFR=(UPROJ-U2PG)/QSS2G
GOTO 310
C * * * * *
C *
C * * * * * CONDITION 4 *
C * * * * * * * * * * * * * * * * * * * * * * * * * * * *
C * VEHICLE CHOKED, SECOND SHOCK BEHIND VEHICLE. *
C * * * * * * * * * * * * * * * * * * * * * * * * * * * *
C
C ITERATION TO FIND FIRST SHOCK STRENGTH (QM1G)
C
500 QM1L=1.0
U2PL=0.0
ZMFL=(UPROJ-U2PL)/SS1
510 CALL ALGST
IF((ABS(ZMF-CRITM)).LT.(CRITM*.001)) GOTO 530
IF (ZMF.GT.CRITM) GOTO 520
QM1R=QM1G
ZMFR=ZMF
GOTO 510
520 QM1L=QM1G
ZMFL=ZMF
GOTO 510
530 USHK1=QM1G*SS1
IF (PUSHK1.EQ.0.0)GOTO 534
CALL SUSHK(USHK1,PUSHK1,DDSHK1)
AVE1=AVE

```

```

DSHK1=DSHK1+DDSHK1
PRINT*, 'AT T= ', 'DSHK1= ', DSHK1
GOTO 535
534 PUSHK1=USHK1
535 SS2=SS1*CA2PA1(QM1G, QM2G)
SST3=SS2*CTSS2(CRITM)
P2=P1*CP2(QM1G, QM2G)
PT3=P2*CTP2(CRITM)
RHO2=RHO1*CP2(QM1G, QM2G)/(CA2PA1(QM1G, QM2G)**2.0)
RHOT3=RHO2*CTRH02(CRITM)
540 SS4=SST3/CTSS2(SCRITM)
PRINT*, 'THREE'
IND=0
U4=SCRITM*SS4
C
C UREL=VELOCITY OF FLOW BEHIND PROJ. RELATIVE TO TUBE
C
C UREL=U4-UPROJ
C
C ITERATION TO FIND SECOND SHOCK STRENGTH (ZM5G)
C
ZM5R=SCRITM
ZM6R=CM2(ZM5R)
U5R=ZM5R*SS4
SS6R=SS4*CA2PA1(ZM5R, ZM6R)
U6R=ZM6R*SS6R
USHKR=U5R-UREL
USABR=USHKR-U6R
ZM5L=1.0
USABL=-UREL
600 TSLOPE=(USABR-USABL)/(ZM5R-ZM5L)
TYO=USABL-(ZM5L*TSLOPE)
ZM5G=(USAB-TYO)/TSLOPE
U5G=ZM5G*SS4
ZM6G=CM2(ZM5G)
SS6G=SS4*CA2PA1(ZM5G, ZM6G)
U6G=ZM6G*SS6G
USHKG=U5G-UREL
USABG=USHKG-U6G
IF((ABS(USABG-USAB)).LT.(USAB*.001))GOTO 620
IF((USABG.GT.USAB)GOTO 610
ZM5L=ZM5G
USABL=USABG
GOTO 600
610 ZM5R=ZM5G
USABR=USABG
GOTO 600
620 USHK2=USHKG
IF(PUSHK2.EQ.0.0)GOTO 630
CALL SUSHK(USHK2, PUSHK2, DDSHK2)
DSHK2=DSHK2+DDSHK2

```

```

PRINT*, 'AT T= ', 'DSHK2= ', DSHK2
GOTO 640
630 DSHK2=DP-PL
PUSHK2=USHK2
640 IF (DSHK1.GT.TL)GOTO 700
P4=PT3/CTP2(SCRITM)
RHO4=RHOT3/CTRHO2(SCRITM)
P6=P4*CP2(ZM5G,ZM6G)
RHO6=RHO4*CP2(ZM5G,ZM6G)/(CA2PA1(ZM5G,ZM6G)**2.)
FSAB=(P6*ASAB)+FRICT
DDS=(.5*(-FSAB/SABM)*(DT**2.))+ (USAB*DT)
USAB=USAB-((FSAB/SABM)*DT)
IF(USAB.LT.0.0)GOTO 800
U3=CRITM*SS2
U4=SCRITM*SS4
FPROJ=((P2+(RHO2*(U3**2.)))-(P4+(RHO4*(U4**2.))))
$ *APROJ
DDP=(.5*(-FPROJ/PROJM)*(DT**2.))+ (UPROJ*DT)
OLDV=UPROJ
UPROJ=UPROJ-((FPROJ/PROJM)*DT)
T=T+DT
DS=DDS+DS
DP=DDP+DP
CALL PDAT
SSE2=SS2
QM1R=QM1G
QSS2G=SS1*CA2PA1(QM1G,QM2G)
U1G=QM1G*SS1
U2G=QM2G*QSS2G
U2PG=U1G-U2G
ZMFR=(UPROJ-U2PG)/QSS2G
GOTO 500

```

C  
C  
C  
C  
C  
C  
C

```

* * * * *
*
* * * * *          CONDITION 5
*
*   APPROXIMATE CALCS. AFTER END DIAPHRAGM BROKEN
* * * * *

```

```

700 TS=T
URAR=SSE2-UREL

```

C  
C  
C  
C  
C  
C  
C

```

* * * * *
*
* * * * *          CONDITION 5A
*
* PROJ. CALCULATIONS AFTER DIAPHRAGM BURSTS UNTIL
* RAREFACTION WAVE HITS.
* * * * *

```

```

TA=TS
DELT=(DSHK1-TL)/AVE1

```

```

DRAR=DELT*URAR
DRAR1=DRAR
UPROJ1=UPROJ
DP1=DP
720 PRINT*, 'AT T= ',TA, ' DRAR= ', TL-DRAR
IF(DP.GE.TL) GOTO 750
C
C
C
WHEN RAREFACTION HITS, ANALYSIS GOES TO SECTION 5B

IF((DRAR+DP).GE.TL) GOTO 730
PRINT*, 'FOUR -A'
FPROJ=FPROJ*(UPROJ**2.0)/(OLDV**2.0)
OLDV=UPROJ
DDP=(.5*(-FPROJ/PROJM)*(DT**2.))+(UPROJ*DT)
UPROJ=UPROJ-((FPROJ/PROJM)*DT)
TA=TA+DT
DP=DP+DDP
DRAR=(URAR*DT)+DRAR
PRINT*, ' '
PRINT*, 'T= ',TA
PRINT*, 'UPROJ=',UPROJ
PRINT*, 'DP= ',DP
PRINT*, 'DRAR= ', TL-DRAR
PRINT*, ' '
GOTO 720

C
C
C
C
C
C
* * * * *
*
* CONDITION 5B
* * * * *
* PROJ. CALCULATIONS AFTER RAREFACTION WAVE HITS
* * * * *
730 TB=TA
DIST=(TL-DP)
IF(DIST.LE.1.0) DIST=1.0
740 FPROJ=FPROJ-(FPROJ*UPROJ*(TB-TA)/DIST)
IF (FPROJ.LE.0.0) FPROJ=0.0
DDP=(.5*(-FPROJ/PROJM)*(DT**2.))+(UPROJ*DT)
UPROJ=UPROJ-((FPROJ/PROJM)*DT)
TB=TB+DT
DP=DP+DDP
DRAR=(URAR*DT)+DRAR
PRINT*, ' '
PRINT*, 'FOUR-B'
PRINT*, 'T= ',TB
PRINT*, 'UPROJ=',UPROJ
PRINT*, 'DP= ',DP
PRINT*, 'DRAR= ', TL-DRAR
IF(DP.GE.TL)GOTO 750
GOTO 740
C

```

```

C      * * * * *
C      *
C      * * * * *          CONDITION 5C
C      * * * * *          *
C      * SABOT ANALYSIS AFTER END DIAPHRAGM BROKEN UNTIL *
C      * SABOT SHOCK HITS RAREFACTION WAVE.
C      * * * * *          *
C      * * * * *          *
C      IND=0 --- ANALYSIS CAME FROM CONDITIONS 1K OR 4
C      IND=1 --- ANALYSIS CAME FROM CONDITION 3
C      IND=2 --- ANALYSIS CAME FROM CONDITION 2
C
750  DRAR=DRAR1
      PUSHK2=0.0
      IF(IND.EQ.0)GOTO 754
      IF(IND.EQ.1)GOTO 751
      PUSHK2=PUSHK1
      DSHK2=DSHK1
      UREL=0.0
      SS4=SS1
      PT3=P1*CTP2(0.0)
      GOTO 754
751  USHK2=UPROJ1
      DSHK2=DP1-PL
      PUSHK2=USHK2
      UREL=0.0
      P4=PT5/CTP2(GGM4)
      SS4=SST3/CTSS2(GGM4)
      ZM5R=5.0
      U5R=ZM5R*SS4
      ZM6R=CM2(ZM5R)
      SS6R=SS4*CA2PA1(ZM5R,ZM6R)
      U6R=ZM6R*SS6R
      USABR=U5R-U6R
      GOTO 755
C
C      ITERATION TO FIND SABOT SHOCK STRENGTH (ZM5G)
C
754  ZM5R=ZM5G
      USABR=USHKG
      P4=PT3/CTP2(SCRITM)
755  ZM5L=1.0
      USABL=-UREL
C
C      WHEN SABOT HITS RAREFACTION WAVE, ANALYSIS GOES
C      TO CONDITION 5D
C
756  IF((DSHK2+DRAR).GE.TL)GOTO 770
      TSLOPE=(USABR-USABL)/(ZM5R-ZM5L)
      TYO=USABL-(ZM5L*TSLOPE)
      ZM5G=(USAB-TYO)/TSLOPE
      U5G=ZM5G*SS4

```

```

ZM6G=CM2(ZM5G)
SS6G=SS4*CA2PA1(ZM5G,ZM6G)
U6G=ZM6G*SS6G
USHKG=U5G-UREL
USABG=USHKG-U6G
IF((ABS(USABG-USAB)).LT.(USAB*.001))GOTO 758
IF(USABG.GT.USAB)GOTO 757
ZM5L=ZM5G
USABL=USABG
GOTO 756
757 ZM5R=ZM5G
USABR=USABG
GOT 756
758 USHK2=USHKG
IF(PUSHK2.EQ.0.0) GOTO 760
CALL SUSHK(USHK2,PUSHK2,DDSHK2)
DSHK2=DSHK2+DDSHK2
PRINT*,'AT T ',T,'DSHK2= ',DSHK2
GOTO 765
760 PUSHK2=USHK2
765 P6=P4*CP2(ZM5G,ZM6G)
FSAB=(P6*ASAB)+FRICT
DDS=(.5*(-FSAB/SABM)*(DT**2.))+(USAB*DT)
USAB=USAB-((FSAB/SABM)*DT)
DRAR=DRAR+(URAR*DT)
T=T+DT
DS=DDS+DS
PRINT*,' '
PRINT*,'FOUR-C'
PRINT*,'T= ',T
PRINT*,'USAB=',USAB
PRINT*,'DS= ',DS
PRINT*,' '
IF (USAB.LT.0.0) GOTO 800
ZM5R=ZM5G
USABR=USABG
GOTO 755

```

```

C
C   CONDITION 5C ANALYSIS IF FROM CONDITION 1
C

```

```

767 IF (KOUNT.GT.1) GOTO 768
URAR=SS1
DELT=(DP-TL)/AVE1
DRAR=URAR*DELT
DP=100.

```

```

C
C   SINCE THE PROJECTILE IS NOW OUT OF THE TUBE, THERE
C   IS NO MORE INTEREST IN IT. BUT, THE ALGORITHM
C   FROM CONDITION 1 IS USED HERE, SO DP WILL STILL BE
C   PRINTED OUT. IT SHOULD THEREFORE BE IGNORED FROM
C   NOW ON.

```

```

C
PRINT*, '*****'
PRINT*, '          IGNORE FURTHER DPS          '
PRINT*, '*****'
KOUNT=2
GOTO 192
768 DRAR=DRAR+(URAR*DT)
    IF((DRAR+DSHK1).GE.TL) GOTO 770
    GOTO 192

C
C
C * * * * *
C *
C *             CONDITION 5D
C * * * * *
C * APPROXIMATE ANALYSIS AFTER SABOT SHOCK AND
C * RAREFACTION WAVE INTERACT.
C * * * * *
C * * * * *
C

770 FSAB=FSAB-FRICT
    TO=T
    DIST=(TL-DS)
    IF(DIST.LE.1.0) DIST=1.0
780 FSAB=FSAB-(FSAB*USAB*(T-TO)/DIST)
    IF (FSAB.LE.0.0)FSAB=0.0
    DSAB=FSAB+FRICT
    DDS=(.5*(-DSAB/SABM)*(DT**2.))+ (USAB*DT)
    USAB=USAB-((DSAB/SABM)*DT)
    DS=DS+DDS
    T=T+DT
    PRINT*, ' '
    PRINT*, 'FOUR-D'
    PRINT*, 'T= ', T
    PRINT*, 'USAB= ', USAB
    PRINT*, ' '

C
C
C WHEN SABOT EXITS TUBE, ANALYSIS STOPS

    IF(DS.GE.TL)GOTO 800
    IF(USAB.LT.0.0) GOTO 800
    GOTO 780
800 CALL EXIT
    STOP
    END

C
C
C SUBROUTINE ALGOI(SS1,ZM1L,ZM1R)
C SUBROUTINE HELPS IN ITERATION
COMMON/A/GAM,GM1,GPI
COMMON/B/USABR,USABL,SS2G,ZM1G,ZM2G,USABG
COMMON/H/USAB,UPROJ
SLOPE=(USABR-USABL)/(ZM1R-ZM1L)

```



```

YO=USABL-(ZM1L*SLOPE)
ZM1G=(USAB-YO)/SLOPE
U1G=ZM1G*SS1
ZM2G=CM2(ZM1G)
SS2G=SS1*CA2PA1(ZM1G,ZM2G)
U2G=ZM2G*SS2G
USABG=U1G-U2G
RETURN
END

```

C  
C

```

SUBROUTINE ALGMC
SUBROUTINE HELPS IN ITERATION
COMMON/A/GAM,GM1,GPI
COMMON/C/ARR,ARL,SMR,SML,ARG,SMG
COMMON/F/AR
SLOPE=(ARR-ARL)/(SMR-SML)
YO=ARL-(SML*SLOPE)
SMG=(AR-YO)/SLOPE
ARG=CAR(SMG)
RETURN
END

```

C  
C

```

SUBROUTINE ALGST
SUBROUTINE HELPS IN ITERATION
COMMON/A/GAM,GM1,GPI
COMMON/D/SS1,ZMFR,ZMFL,QM1R,QM1L,QM1G,QM2G,ZMF,CRITM
COMMON/H/USAB,UPROJ
SLOPE=(ZMFR-ZMFL)/(QM1R-QM1L)
YO=ZMFL-(QM1L*SLOPE)
QM1G=(CRITM-YO)/SLOPE
U1G=QM1G*SS1
QM2G=CM2(QM1G)
QSS2G=SS1*CA2PA1(QM1G,QM2G)
U2G=QM2G*QSS2G
U2PG=U1G-U2G
ZMF=(UPROJ-U2PG)/QSS2G
RETURN
END

```

C  
C

```

SUBROUTINE ZITAR(GAR,GGM4,L)
SUBROUTINE HELPS IN ITERATION
COMMON/A/GAM,GM1,GPI
COMMON/D/SS1,ZMFR,ZMFL,QM1R,QM1L,QM1G,QM2G,ZMF,CRITM
COMMON/F/AR
COMMON/E/SCRITM
IF(L.GT.1)GOTO 50
GGM4L=1.0
GGM4R=SCRITM

```

```

        GOTO 60
50    GGM4L=CRITM
        GGM4R=1.0
60    GARR2=CAR(GGM4R)
        GARL2=CAR(GGM4L)
100   SLOPE=(GARR2-GARL2)/(GGM4R-GGM4L)
        YO=GARL2-(GGM4L*SLOPE)
        GGM4=(GAR-YO)/SLOPE
        GGAR=CAR(GGM4)
        IF((ABS(GGAR-GAR)).LT.(.001*GAR)) GOTO 120
        IF (GGAR.LT.GAR) GOTO 110
        GG4L=GGM4
        GARL2=GGAR
        GOTO 100
110   GGM4R=GGM4
        GARR2=GGAR
        GOTO 100
120   J=0
        RETURN
        END

C
C
        SUBROUTINE SUSHK(U1,P1,D1)
C    SUBROUTINE CALCULATES AVERAGE SHOCK VELOCITY
C    AND NEW SHOCK POSITION.
        COMMON/I/DT
        COMMON/J/AVE
        AVE=(U1+P1)/2
        D1=AVE*DT
        P1=U1
        RETURN
        END

C
C
        SUBROUTINE PDAT
C    PRINTS PERTINENT DATA
        COMMON/G/T,DS,DP
        COMMON/H/USAB, UPROJ
        PRINT*,' '
        PRINT*,' UPROJ= ',UPROJ
        PRINT*,' USAB= ',USAB
        PRINT*,' T= ',T
        PRINT*,' DS= ',DS
        PRINT*,' DP= ',DP
        PRINT*,' '
        RETURN
        END

C
C
        FUNCTION CM2(CM1)
C    CALCULATES MACH NO. BEHIND SHOCK

```

```

COMMON/A/GAM,GM1,GP1
CM2=SQRT((GM1*CM1**2.0+2.0)/(2.0*GAM*CM1**2.0-GM1))
RETURN
END

```

C  
C

```

FUNCTION CA2PA1(CM1,CM2)
CALCULATES SPEED OF SOUND RATIO ACROSS SHOCK
COMMON/A/GAM,GM1,GP1
CA2PA1=SQRT((2.0+GM1*CM1**2.0)/(2.0+GM1*CM2**2.0))
RETURN
END

```

C  
C

```

FUNCTION CP2(CM1,CM2)
CALCULATES STATIC PRESSURE RATIO ACROSS SHOCK
COMMON/A/GAM,GM1,GP1
CP2=(1.0+GAM*CM1**2.0)/(1+GAM*CM2**2.0)
RETURN
END

```

C  
C

```

FUNCTION CAR(SM)
CALCULATES AREA RATIO
COMMON/A/GAM,GM1,GP1
CAR=(1./SM)*(((2./GP1)*(1.+(GM1*.5*(SM**2.))))**
$ (GP1/(2.*GM1)))
RETURN
END

```

C  
C

```

FUNCTION CTSS2(CM)
CALCULATES STAGNATION SPEED OF SOUND RATIO ACROSS SHOCK
COMMON/A/GAM,GM1,GP1
CTSS2=SQRT(1.+((GM1/2.)*(CM**2.)))
RETURN
END

```

C  
C

```

FUNCTION CTP2(CM)
CALCULATES STAGNATION PRESSURE RATIO ACROSS SHOCK
COMMON/A/GAM,GM1,GP1
CTP2=(1.+(.5*GM1*(CM**2.)))*(GAM/GM1)
RETURN
END

```

C  
C

```

FUNCTION CTRHO2(CM)
CALCULATES STAGNATION DENSITY RATIO ACROSS SHOCK
COMMON/A/GAM,GM1,GP1
CTRHO2=(1.+(.5*GM1*(CM**2.)))*(1./GM1)

```

RETURN  
END